



Telethonin Deficiency Is Associated With Maladaptation to Biomechanical Stress in the Mammalian Heart

Ralph Knöll, Wolfgang A. Linke, Peijian Zou, Snjezana Miocic, Sawa Kostin, Byambajav Buyandelger, Ching-Hsin Ku, Stefan Neef, Monika Bug, Katrin Schäfer, Gudrun Knöll, Leanne E. Felkin, Johannes Wessels, Karl Toischer, Franz Hagn, Horst Kessler, Michael Didié, Thomas Quentin, Lars S. Maier, Nils Teucher, Bernhard Unsöld, Albrecht Schmidt, Emma J. Birks, Sylvia Gunkel, Patrick Lang, Henk Granzier, Wolfram-Hubertus Zimmermann, Loren J. Field, Georgine Faulkner, Matthias Dobbelstein, Paul J.R. Barton, Michael Sattler, Matthias Wilmanns and Kenneth R. Chien

Circulation Research 2011, 109:758-769: originally published online July 28, 2011 doi: 10.1161/CIRCRESAHA.111.245787

Circulation Research is published by the American Heart Association. 7272 Greenville Avenue, Dallas, TX 72514

Copyright © 2011 American Heart Association. All rights reserved. Print ISSN: 0009-7330. Online ISSN: 1524-4571

The online version of this article, along with updated information and services, is located on the World Wide Web at:

http://circres.ahajournals.org/content/109/7/758

Data Supplement (unedited) at: http://circres.ahajournals.org/content/suppl/2011/07/28/CIRCRESAHA.111.245787.DC1.html

Subscriptions: Information about subscribing to Circulation Research is online at http://circres.ahajournals.org//subscriptions/

Permissions: Permissions & Rights Desk, Lippincott Williams & Wilkins, a division of Wolters Kluwer Health, 351 West Camden Street, Baltimore, MD 21202-2436. Phone: 410-528-4050. Fax: 410-528-8550. E-mail:

journalpermissions@lww.com

Reprints: Information about reprints can be found online at

http://www.lww.com/reprints

Molecular Medicine

Telethonin Deficiency Is Associated With Maladaptation to Biomechanical Stress in the Mammalian Heart

Ralph Knöll, Wolfgang A. Linke, Peijian Zou, Snježana Miočić, Sawa Kostin,
Byambajav Buyandelger, Ching-Hsin Ku, Stefan Neef, Monika Bug, Katrin Schäfer, Gudrun Knöll,
Leanne E. Felkin, Johannes Wessels, Karl Toischer, Franz Hagn, Horst Kessler, Michael Didié,
Thomas Quentin, Lars S. Maier, Nils Teucher, Bernhard Unsöld, Albrecht Schmidt, Emma J. Birks,
Sylvia Gunkel, Patrick Lang, Henk Granzier, Wolfram-Hubertus Zimmermann, Loren J. Field,
Georgine Faulkner, Matthias Dobbelstein, Paul J.R. Barton, Michael Sattler,
Matthias Wilmanns, Kenneth R. Chien

Rationale: Telethonin (also known as titin-cap or t-cap) is a 19-kDa Z-disk protein with a unique β-sheet structure, hypothesized to assemble in a palindromic way with the N-terminal portion of titin and to constitute a signalosome participating in the process of cardiomechanosensing. In addition, a variety of telethonin mutations are associated with the development of several different diseases; however, little is known about the underlying molecular mechanisms and telethonin's in vivo function.

<u>Objective:</u> Here we aim to investigate the role of telethonin in vivo and to identify molecular mechanisms underlying disease as a result of its mutation.

Methods and Results: By using a variety of different genetically altered animal models and biophysical experiments we show that contrary to previous views, telethonin is not an indispensable component of the titin-anchoring system, nor is deletion of the gene or cardiac specific overexpression associated with a spontaneous cardiac phenotype. Rather, additional titin-anchorage sites, such as actin–titin cross-links via α-actinin, are sufficient to maintain Z-disk stability despite the loss of telethonin. We demonstrate that a main novel function of telethonin is to modulate the turnover of the proapoptotic tumor suppressor p53 after biomechanical stress in the nuclear compartment, thus linking telethonin, a protein well known to be present at the Z-disk, directly to apoptosis ("mechanoptosis"). In addition, loss of telethonin mRNA and nuclear accumulation of this protein is associated with human heart failure, an effect that may contribute to enhanced rates of apoptosis found in these hearts.

<u>Conclusions:</u> Telethonin knockout mice do not reveal defective heart development or heart function under basal conditions, but develop heart failure following biomechanical stress, owing at least in part to apoptosis of cardiomyocytes, an effect that may also play a role in human heart failure. (*Circ Res.* 2011;109:758-769.)

Key Words: genetics ■ mechanosensation ■ mechanotransduction ■ cardiomyopathy ■ heart failure

Original received March 30, 2011; revision received July 15, 2011; accepted July 20, 2011. In June 2011, the average time from submission to first decision for all original research papers submitted to *Circulation Research* was 14.48 days.

From the Imperial College, National Heart & Lung Institute, British Heart Foundation, Centre for Research Excellence, Myocardial Genetics, London, UK (R.K., B.B., S.N., J.W., L.S.M., N.T., B.U., A.S., S.G.); Institute of Physiology, Department of Cardiovascular Physiology, Ruhr University Bochum, Bochum, Germany (W.A.L.); Göttinger Zentrum für Molekulare Biologie, Georg-August-University Göttingen, Germany (M.B., M.D.); CRIBI, University of Padua, Padua, Italy (S.M., G.F.); EMBL Hamburg, DESY, Hamburg, Germany (P.Z., M.W.); Department of Pharmacology, Georg-August-University Göttingen Göttingen Göttingen, Germany (M.D., W.-H.Z.); Department of Pediatric Cardiology, Georg-August-University Göttingen (T.Q.); Department of Cardiology and Pneumology, Georg-August-University Göttingen (K.S., K.T., L.J.F.); Physiology and Biophysics Unit, University of Münster, Münster, Germany (P.L.); Department of Physiology, University of Arizona, Tucson (H.G.); Institute of Structural Biology, Helmholtz Zentrum München, Neuherberg, Germany (P.Z., M.S.); Center for Integrated Protein Science, Department Chemie, Technische Universität München, Garching, Germany (P.Z., F.H., H.K., M.A.); Institute for Advanced Study, Department Chemie, Technische Universität München (F.H., H.K.); Harvard Stem Cell Institute, Harvard Medical School, Boston, Boston, MA (K.R.C.); University of California at San Diego, Department of Molecular Medicine, La Jolla, CA (R.K.); Heart Centre, Georg-August-University Göttingen (R.K., C.-H.K., G.N.); Max-Planck-Institute for Heart and Lung Research, Bad Nauheim, Germany (S.K.); Heart Science Centre, National Heart and Lung Institute, Imperial College, Harefield Middlesex, UK (L.E.F., E.J.B., P.J.R.B.); NIHR Cardiovascular Biomedical Research Unit, Royal Brompton and Harefield NHS Foundation Trust, London (P.J.R.B.); Chemistry Department, Faculty of Science, King Abdulaziz University, Jeddah, Saudi Arabia (HK.).

Correspondence to Professor Ralph Knöll, MD, PhD, Chair, Myocardial Genetics, National Heart & Lung Institute, British Heart Foundation—Centre for Research Excellence, Imperial College, South Kensington Campus, Flowers Building, 4th floor, London SW7 2AZ, UK. E-mail r.knoell@imperial.ac.uk

© 2011 American Heart Association, Inc.

Circulation Research is available at http://circres.ahajournals.org

The heart is a dynamic organ capable of self-adaptation to ▲ mechanical demands, but the underlying molecular mechanisms remain poorly understood. We have previously shown that the sarcomeric Z-disk, which serves as an important anchorage site for titin and actin molecules, not only is important for mechanical force transduction but also harbors a pivotal mechanosensitive signalosome in which muscle LIM protein (MLP) and telethonin play major roles in the perception of mechanical stimuli. 1-3 Here we focus on telethonin, a striated-muscle-specific protein with a unique β-sheet structure (and no direct homologue genes), enabling it to bind in an antiparallel (2:1) sandwich complex to the titin Z1-Z2 domains, essentially "gluing" together the N-termini of 2 adjacent titin molecules.4 Interestingly, the telethonintitin interaction represents the strongest protein-protein interaction observed to date.5 Besides being phosphorylated by protein kinase D,6 telethonin is also an in vitro substrate of the titin kinase, an interaction thought to be critical during myofibril growth.7 The giant elastic protein titin extends across half the length of a sarcomere and is thought to stabilize sarcomere assembly by serving as a scaffold to which other contractile, regulatory, and structural proteins

Telethonin was shown to interact with MLP, hypothesized to be part of a macromolecular mechanosensor complex and to play a role in a subset of human cardiomyopathies.² In this context, telethonin interacts with calsarcin-1 (also known as FATZ-2 or myozenin-2, a gene recently shown to cause cardiomyopathy9), ankyrin repeat protein 2, small ankyrin-1 (a transmembrane protein of the sarcoplasmic reticulum), 10 and minK (a potassium channel β subunit). 11-14 In addition, telethonin was shown to interact with MDM215 and MuRF1,¹⁶ E3 ubiquitin ligases with strong impact on cardiac protein turnover as well as with the proapoptotic protein Siva.¹⁷ Recessive nonsense mutations in the telethonin gene are associated with limb-girdle muscular dystrophy type 2 G^{18–20} and heterozygous missense mutations with dilated and hypertrophic forms of cardiomyopathy^{1,21,22} as well as with intestinal pseudo-obstruction.²³ Interestingly, a naturally occurring telethonin variant that has a Glu13 deletion (E13del telethonin) was initially found in patients affected by hypertrophic cardiomyopathy²¹ and then later in healthy, unaffected individuals.^{24,25} However, the molecular consequences of the E13del variant, especially on the telethonin-titin interaction, as well as telethonin mediated pathways in general remain unclear.

Methods

Please see also the detailed methods description in the Online Supplemental material, available at http://circres.ahajournals.org.

Sarcomere Stretch and Titin Localization

Myofibrils were prepared from telethonin-deficient or wildtype tissue as described previously. 26

In Vitro Protein Interaction Assay

Z1Z2 titin, MLP, telethonin, and its mutants were expressed and purified as previously described.²⁷ Z1Z2–telethonin complexes were formed and analyzed on native gels and gel filtration columns as previously described.^{4,27}

Non-Standard Abbreviations and Acronyms

 α -MHC alpha myosin heavy chain beta myosin heavy chain ANF atrial natriuretic factor BNP brain natriuretic peptide dn dominant negative NLS nuclear localization sequence

P53DBD p53 DNA binding domain
SERCA sarcoplasmic reticulum ATPase

NMR Spectroscopy

U-²H, ¹⁵N-labeled p53DBD for NMR studies was prepared using M9-medium supplemented with 1g/L ¹⁵NH₄Cl, 2g/L ²H, ¹³C glucose in 99.9% D₂O (Eurisotop, Saarbrücken, Germany). Nuclear magnetic resonance (NMR) experiments were done at 293K on a Bruker Avance900 spectrometer (Bruker Biospin, Rheinstetten, Germany).

Antibodies

In the current project we used 2 different antitelethonin antibodies: a mouse antitelethonin polyclonal antibody raised against a recombinant His-tagged human full-length telethonin (Western blots, immune precipitations, mouse heart, and human heart sections) and a rat polyclonal antitelethonin antibody (immunofluorescence in neonatal rat cardiac myocytes). Both the mouse and rat antibodies to human telethonin were produced by immunizing, respectively, Balb/C mice or LOU/Nmir rats with purified recombinant full-length telethonin protein (1 to 167 aa), and their specificity was checked by their ability to detect telethonin on Western blots of human heart and skeletal muscle protein. Anti-Z1Z2 titin antibody was a kind gift of Prof. S. Labeit. We used as well p21WAF1 EA10 (Calbiochem), Mdm2 2A9 and 2A10, myc 4A6 (Upstate) and actin AC15 (Abcam), antip53 (DO-1, FL 393, Santa Cruz), and mouse monoclonal p53 (1C12, Cell signaling), mouse monoclonal anti α -actinin (Sigma), and phalloidin conjugated Alexa 350 antibody. The secondary antibodies used were Alexa-abeled 633 antirat, Alexa-labeled 488 antirabbit, and Alexa-labeled 488 antimouse (Invitrogen) antibody (please see also the Online Supplemental Material for additional information).

Statistics

All animals used in the experiments were matched on age and sex. All assays were analyzed in "double-blind" fashion. T tests were used to analyze differences in echocardiography (n=8 to 9 animals per group) and for the analysis of Z-disks following sarcomere stretch. Whenever more than 2 groups were compared, analysis of variance (ANOVA) tests followed by Bonferroni's Multiple Comparison test were applied. Statistical significance was reached at P<0.05.

Results

To be able to perform a detailed functional analysis of cardiac performance, we generated telethonin-deficient mice by homologous recombination, replacing exons 1 and 2 with a Lac Z-neomycin cassette (Figure 1). Using this approach, telethonin was found to be transcribed as early as embryonic day 10.5 (not shown). Telethonin is a late-in protein; as such, it is not a surprise that telethonin-deficient mice are born in the expected Mendelian ratios and that this protein is apparently not required during heart development.^{28,29}

In contrast to recently published zebrafish and xenopus knock-down models^{30,31} as well as what was expected on the

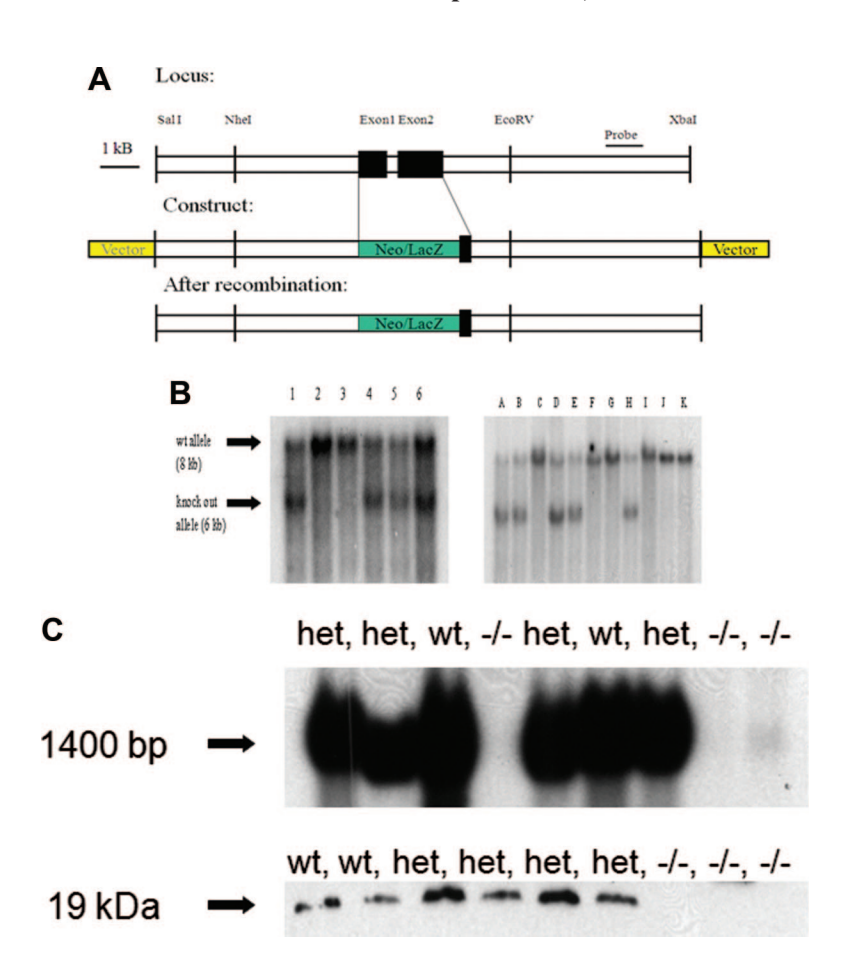


Figure 1. Generation of telethonin $^{-/-}$ animals. A, General strategy for gene targeting. The gene for telethonin is encoded by 2 exons; restriction sites are indicated. The gene was replaced by a LacZ/Neomycin cassette (targeting construct is indicated). B, Southern hybridization of embryonic stem cells (left panel: different stem cell lines marked 1 to 6) as well as of resulting animals (right panel: different animals marked A-K). C, Telethonin mRNA expression, analyzed by Northern blot (upper row), as well as protein expression, analyzed by Western blotting, indicates that telethonin-/- results in a "true null allele."

basis of the available knowledge, the analysis of myocardial function by echocardiography (Online Table I) as well as by in vivo heart catheterization using 3- to 4-month-old telethonin^{-/-} mice under basic conditions did not reveal any abnormal parameters. Histological analysis of the spontaneous cardiac phenotype of telethonin^{-/-} mice revealed no alterations, including the amount of extracellular matrix deposition, (see next paragraph), and changes in titin-isoform composition that could be excluded on the basis of gel electrophoresis (Online Figure I). Epifluorescence experiments showed unaltered global intracellular Ca²⁺ handling (Online Figure II) and immunohistochemistry as well as immunogold electron microscopy did not reveal any defects in telethonin-deficient Z-disks (Online Figure III).

Telethonin was shown to interact directly with the potassium channel subunit minK,13 as well as with different sodium channels such as SCN5A²³; as a consequence, we performed extensive analyses of electrocardiograms (ECG) in vivo as well as patch-clamp experiments in vitro, but did not find any significant differences in ECG parameters such as PQ interval, QRS width, QT interval, or action-potential repolarization between control littermates and telethonindeficient animals, without any occurrence of early or delayed after depolarizations in either group. The telethonin-minK or telethonin-SCN5A interaction may thus have little physiological relevance in the heart, at least in the mouse model (Online Figure IV). This remarkable mild cardiac phenotype despite loss of telethonin is supported by another recently published study of telethonin knock-out mouse, in which the same approach has been used to inactivate telethonin (ie, exons 1 and 2 have been replaced by a Lac Z neomycin cassette) and in which the skeletal muscle phenotype has been analyzed but almost no pathology has been detected under spontaneous conditions.32

Telethonin was shown to interact with the N-terminal Z1Z2 titin and, as such, might have an important function in mechanically linking 2 titin molecules together.⁴ Again, surprisingly from what we expected, a stretch of single isolated myofibrils obtained from telethonin^{-/-} heart or skeletal muscle did not cause any changes in Z-disk architecture or displacement of the titin N-terminus from the Z-disk, even when the sarcomeres were extended stepwise to (unphysiological) lengths of $>3.2 \mu m$ to reach very high passive forces of tens of mN/mm² (Figure 2A and 2B). In contrast, compromised anchorage of the titin N-terminus was observed after removal of actin from cardiac sarcomeres (using a Ca²⁺-independent gelsolin fragment²⁶), suggesting that telethonin is mechanically relevant only when there is additional disturbance of the Z-disk (Figure 2A and 2B), such as impairment of the α -actinin-mediated titin-actin cross-links.

Moreover, we reconstituted in vitro a complex consisting of telethonin and the N-terminal (Z1-Z2) titin domains and analyzed the effects of different human telethonin mutations on this complex formation. In contrast to several point mutations tested previously,4 the E13del variant, which because of its presence in healthy unaffected individuals has been regarded as a polymorphism^{24,25} rather than a disease-

Figure 2. Probing functional consequences of telethonin deficiency at the subcellular and organismic levels. A and B, Myofibrils were isolated from either wildtype (WT) or homozygous telethonin-deficient (KO) mouse hearts and stretched to a desired sarcomere length (SL) under nonactivating conditions. Then, myofibrils were stained with an antibody to the telethonin-binding titin domains, Z1-Z2, and the secondary ones labeled using FITC-conjugated IgG. A, Phase-contrast (pc) and immunofluorescence (Z1Z2) images of stretched myofibrils from cardiac muscle before actin extraction; telethonin-deficient skeletal muscle; and cardiac muscle after actin extraction using a Ca²⁺-independent gelsolin fragment (shown are myofibrils at 2 different stretch states). Scale bar, 2 µm. B, (top) Quantitation of the broadness of the titin label in the Z-disk by determining the full width at half-maximum (FWHM) peak height on intensity profiles along the myofibril axis. (bottom) Average widths of Z1Z2-titin label in WT and KO cardiac myofibrils at different SLs, before and after actin extraction. Data are means \pm SD (n=3 to 6). *P<0.05 in Student t test. **C**, Pull-down with MLP. N-terminus of titin (Z1Z2, used as a control), Tel (1 to 90), Tel (1 to 90, dE13), Tel (1 to 90, E13A), Tel (1 to 90, E13R), and Tel (1 to 90, E13W) were incubated with a recombinant GST-MLP fusion protein and pulled down with glutathione-sepharose 4B beads (anti-GST antibody antirabbit, Pharmacia Biotech, Sweden). D, Pull-down with Z1Z2. Same experiment as in C, except that instead of MLP an H-tagged N-terminus of titin Z1Z2 was used (pull down with Ni2+-NTA beads (QIAGEN, Germany), blot with antibody against telethonin). E, Native PAGE analysis of titin/telethonin complexes formed from telethonin and its mutants with Z1Z2. On the native gel, only the Z1Z2telethonin complex and Z1Z2 were visible. F, Analysis of the Z1Z2-telethonin complex formation by size exclusion chromatography in combination with static light scattering. The complexes were loaded onto a sephadex column, molecular masses were calculated to be 23.0 (Z1Z2) and 55.4 (Z1Z2-telethonin complex) kDa. G, Structure of the telethonin-titin Z1-Z2 complex, the arrow indicates glutamate 13 (E13), important for stabilizing the β -hairpin structure. H, Functional analysis of telethonin deficiency in vivo: 2 to 3 weeks after transverse aortic constriction (TAC), telethonin^{-/-} animals developed a defect in myocardial function (increased end-systolic and enddiastolic diameters, decrease in fractional shortening as well as increased left ventricular mass [LVM] and LVM per body mass [*P<0.05, **P<0.01], error bars indicate standard error of the mean [SEM]).

50

0.2

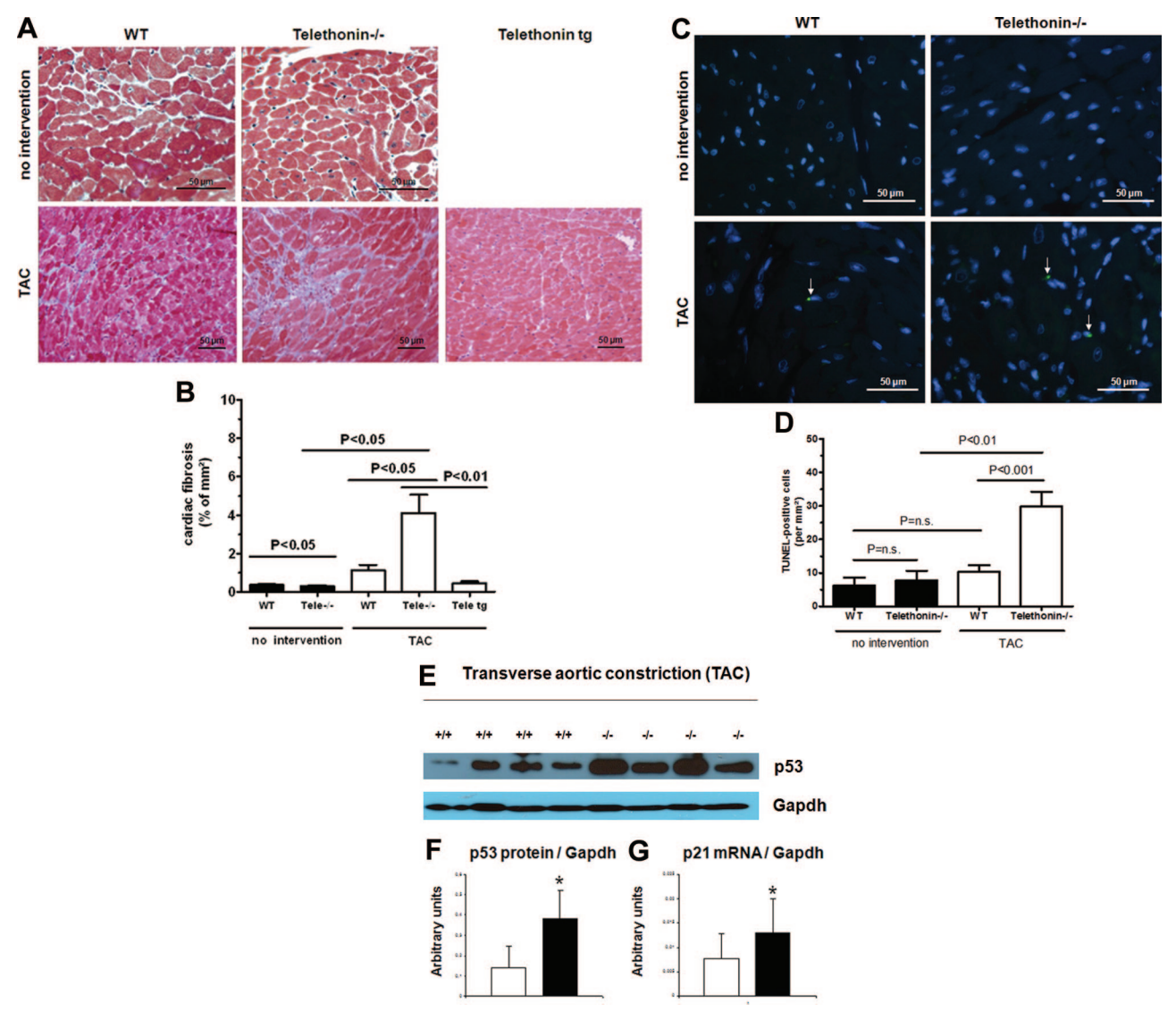


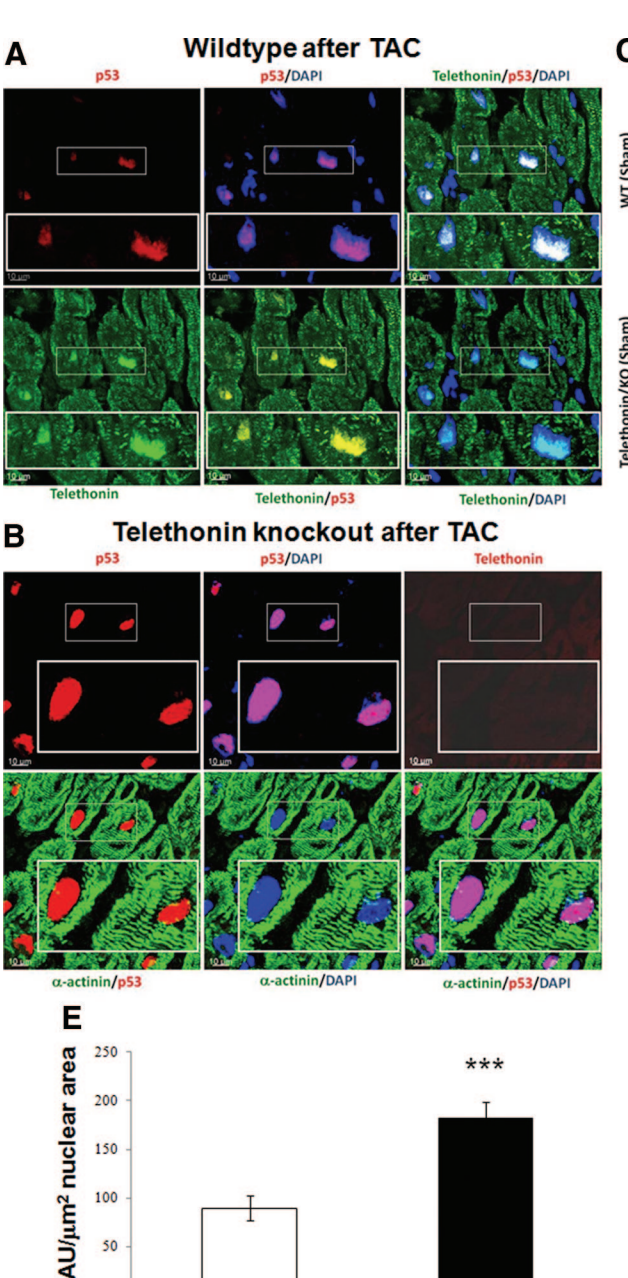
Figure 3. Telethonin—analysis of fibrosis, apoptosis, and p53. A, Wildtype (WT) and telethonin knockout (KO) hearts were analyzed for the presence of fibrosis (masson trichrome stain) without intervention and after transverse aortic constriction (TAC). Telethonin transgenic animals did not develop any significant increase in fibrosis. B, Quantification of fibrosis; note the significant increase in fibrosis in the telethonin-deficient animals (without intervention [solid bars] and after TAC [open bars]; error bars indicate standard deviation [SD]). C, Wildtype (WT) and telethonin knockout (KO) hearts were analyzed for the presence of apoptosis without intervention and after transverse aortic constriction (TAC). D, Quantification of apoptosis; note the significant increase in apoptosis in the telethonin-deficient animals (without intervention [solid bars] and after TAC [open bars]; error bars indicate standard deviation [SD]). E, Western blot analysis of p53 expression in hearts of telethonin knockout as well as corresponding wildtype litter mate control hearts. Equal loading of the membrane has been confirmed by GAPDH gene expression. Note the significant increase in p53 expression in the telethonin-franimals. F, Quantification of p53 protein expression. Data have been normalized to GAPDH. Note the significant increase in p53 expression in the telethonin-franimals (n=4 animals per group; open bars: wildtype animals; solid bars: telethonin-franimals.

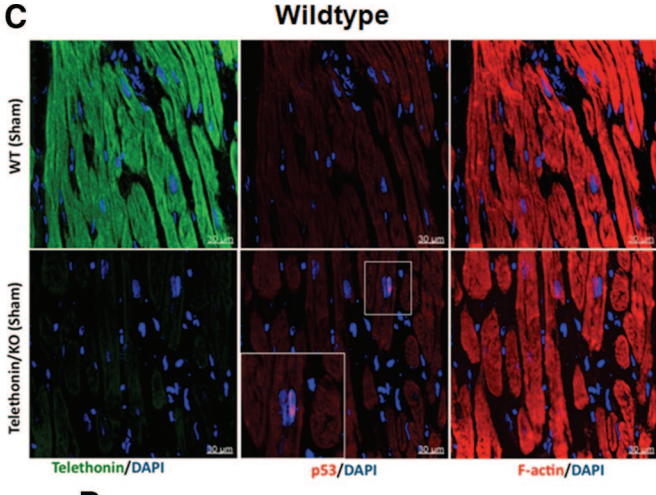
*P<0.05; error bars indicate standard deviation [SD]). G, Relative levels of p21 mRNA transcripts in left ventricles. We used hearts obtained from WT and telethonin-franic subjected to TAC for 3 weeks and analyzed mRNA expression by quantitative real-time PCR. Note the significant increase in p21 gene expression, which is a p53 target gene (open bars: wildtype animals [n=5]; solid bars: telethonin-franimals [n=12]. *P<0.05 against WT-TAC; error bars indicate standard deviation [SD]).

causing mutation, 21 lost the ability to bind the titin N-terminus (Figure 3E through 3H). Consistent with previous data, 4 the deletion of this residue in telethonin leads to a loss of proper formation of the telethonin β -hairpin structure, which forms the basis for the titin binding. Given the available information on heterozygous and homozygous telethonin deficiency reported here and the fact that heterozygous loss of telethonin is not associated with any phenotype (Figure 3H), one possible conclusion is that E13del telethonin is probably a harmless, naturally occurring variant unable to

bind titin, hence supporting our view that telethonin, at least in mammals, performs no important structural functions. However, additional effects of the E13del telethonin variant cannot be excluded, and homozygous patients have not been reported.

The fulminant defects observed after actin removal in the myofibril stretch experiments led us to increase the biomechanical load under in vivo conditions by transverse aortic constriction (TAC). Two to 3 weeks after this intervention, telethonin^{-/-} animals developed maladaptive cardiac hyper-





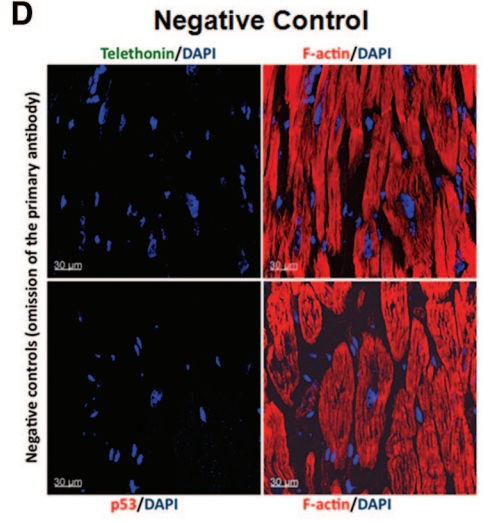


Figure 4. Analysis of telethonin/p53 colocalization. A through D, Representative confocal micrographs showing nuclear localization of p53 in wildtype (WT) (A) and telethonin knockout hearts (B) after TAC. Telethonin and p53 localization has also been analyzed under spontaneous conditions (C); the control panel is provided under D. Note that telethonin is not detectable in telethonindeficient hearts, and in telethonin-deficient animals, just a very few nuclei having an apparent tendency to be positive for p53 were observed (boxed regions). However, this phenomenon was so rare that it does not differ substantially from WT sham-operated mice.

Note as well that in wildtype mice, telethonin is present in the nuclei after TAC, where it colocalizes with p53. Inserts are higher magnifications of the boxed regions (p53 in red, DAPI [nuclear staining] in **blue**, telethonin or α -actinin in **green** mark cardiomyocytes). **E**, It is also evident that p53 nuclear expression levels are much higher in telethonin knockout mice than in wildtype mice after TAC (graph; ***P<0.005; error bars indicate standard deviation [SD]).

Telethonin-/-

trophy and severe heart failure as judged by clinical signs and echocardiography (Figure 3H).

WT

50

Moreover, we found an increase in focal fibrosis as well as a significant increase in TUNEL positive cells in the telethonin^{-/-} animals following the TAC intervention pointing to apoptosis as a possible cause of cell death (Figure 2A through 2D). A detailed analysis revealed that primarily cardiac myocytes were TUNEL positive, and gene expression analysis revealed differential expression of several genes involved in the apoptotic pathway (Online Figures V and VI).

Cardiac apoptosis can be efficiently induced by the tumor suppressor gene product p53,33 a protein known to be polyubiquitinylated and marked for degradation by the E3 ubiquitin ligase MDM2.34 Western blot analysis revealed increased p53 levels in the telethonin^{-/-} animals following TAC (Figure 2E and 2F), whereas the apoptosis repressor with caspase recruitment domain (ARC)—another important heart specific survival factor—remained unchanged (not shown). We also found significant increases in p21 and Caspase 8 mRNA expression, both of which are p53 target genes (Figure 2G, Online Figure VI), and a significant

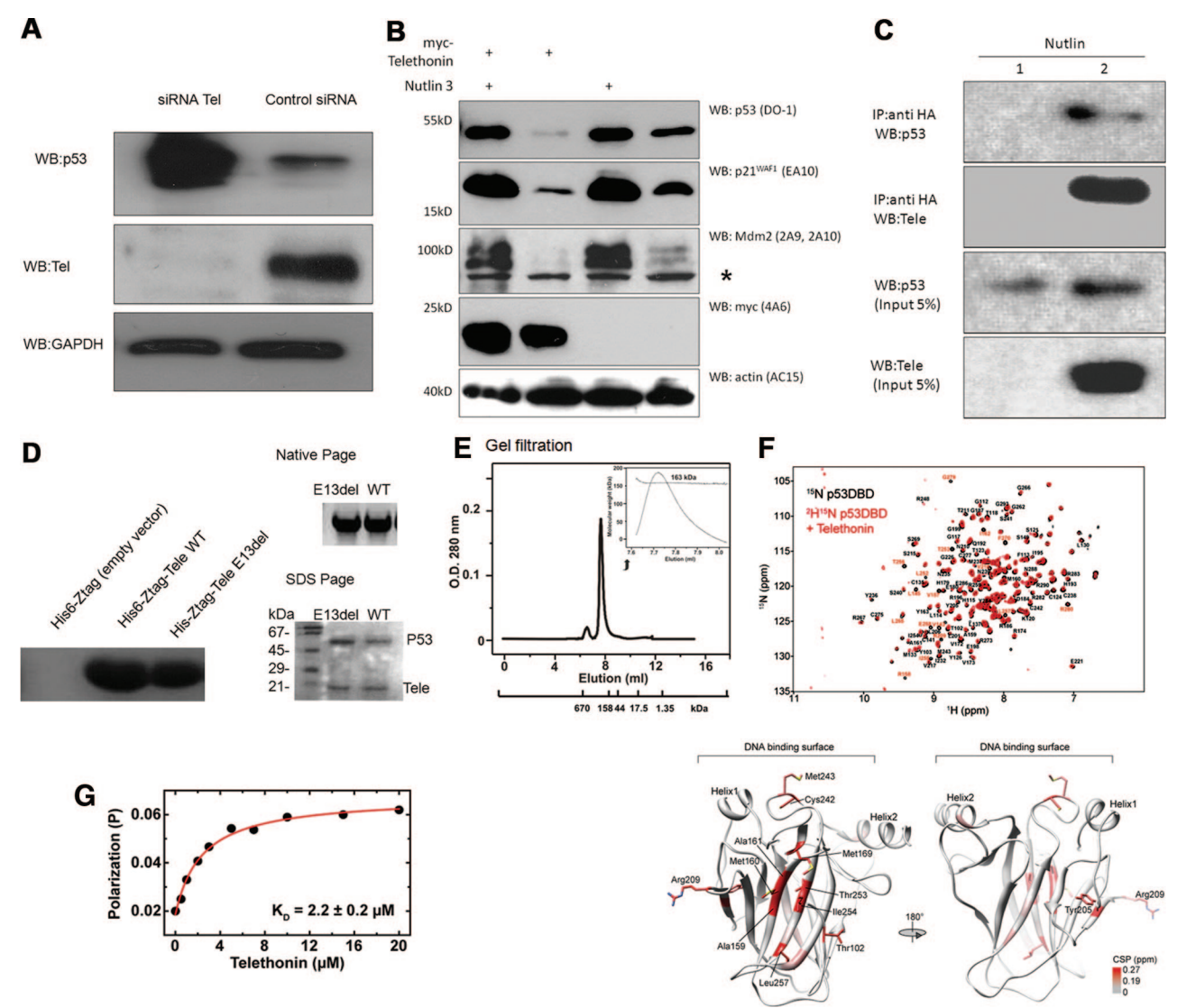


Figure 5. Telethonin/p53 interaction. A, After 48 hours of silencing with siRNA telethonin, neonatal rat cardiomyocytes were incubated with doxorubicin (1 µmol/L) for the next 18 hours. The cells were harvested and whole-cell extracts were used for Western blot analysis. Membranes were probed with mouse polyclonal telethonin as well as with rabbit polyclonal p53 antibodies (Santa Cruz). GAPDH was used as a loading control. Please note the strong induction of p53 when telethonin is knocked down. B, U2OS cells were transfected with myc-telethonin and treated with nutlin-3. Cells were harvested 36 hours posttransfection in RIPA buffer. Cell lysates were used for Western blot analysis. *Unspecific signal. C, Interaction between telethonin and p53. This interaction was detected in U2OS cells between endogenous p53 and transfected HA-tagged telethonin in the presence of Nutlin (8 μmol/L). The IP samples were subjected to SDS-PAGE and blotted and the blot probed with antip53 monoclonal antibody (DO-1, Santa Cruz). Lane 1: U2OS cells transfected with empty plasmid; IP was performed with anti-HA antibody. Lane 2: telethonin transfected U2OS cells; IP was performed with anti-HA antibody. D, Pulldown and complex purification of full-length p53-telethonin complexes. Left: Pull-down experiment using His6-Z-tagged wild type and E13del mutant telethonin and empty His6-Z-tagged vector as a control. Protein complexes were eluted from a Ni-NTA column and analyzed by SDS-PAGE electrophoresis followed by transfer to nitrocellulose membrane. The presence of p53 protein was detected by anti-p53 antibody staining. Right: The elution peaks of complexes formed with wild type or E13del telethonin were analyzed on native PAGE (upper panel) and SDS-PAGE (lower panel). E, Telethonin wildtype or E13del mutant form a complex with the DNA-binding domain of p53 (p53DBD). The complex was separated using size-exclusion chromatography (Superdex 200), and the molecular weight was measured by static light scattering. F, Interaction between p53 DNA-binding domain (DBD) and telethonin. Top panel: Superposition of ¹H, ¹⁵N TROSY experiments of 50 μmol/L ¹⁵N-labeled p53DBD (black) and the complex of ²H, ¹⁵N p53DBD and telethonin **(red)** recorded at 900 MHz proton frequency. Some signals within p53DBD experience substantial line broadening in the complex (red). The signals of many other amino acid residues show chemical shift perturbations on complex formation (black). Bottom panel: CSP values mapped onto the structure of p53DBD. Significantly affected residues are labeled and cluster to one side of the β -barrel region of p53DBD. The p53 DNA-binding region consisting of helix 1 and 2 (H1, H2) and loop 3 (L3) is indicated. Color coding: yellow to red, above mean value plus one standard deviation; red, above mean value plus 2 standard deviations (see also middle panel). G, Fluorescence polarization of 0.5 μ mol/L fluorescein-labeled p53DBD on the addition of telethonin in 10 mmol/L sodium phosphate pH7.2, 1 mmol/L TCEP. Fitting to an apparent 1-site binding model (red line) yields a dissociation constant of 2.2±0.2 µmol/L. Three individual measurements were performed for error estimation.

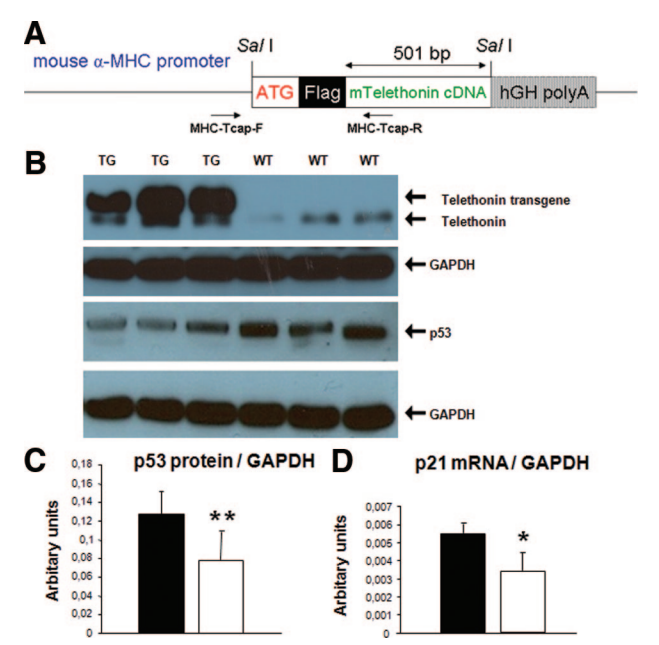
increase in nuclear p53 (Figure 4), supporting the finding of enhanced p53 protein levels.

Interestingly, myostatin has been implicated in the regulation of p53 and p21 expression; it is a negative regulator of cardiac growth^{35–38} and is upregulated under stress.^{39–41} Moreover, myostatin has also been associated with fibrosis.⁴² Most important, telethonin has been shown previously to interact with myostatin and to inhibit its expression.⁴³ Thus myostatin might be able to cause the observed effects, but we did not detect any significant changes in myostatin mRNA or protein expression (Online Figures VII and VIII).

We also performed in vitro experiments in neonatal rat cardiomyocytes, in which we knocked down telethonin and found a strong induction of p53 after additional doxorubicin treatment (a drug known to cause oxidative cellular stress and to induce stress-responsive genes⁴⁴; Figure 5A). In addition, we found evidence of telethonin being present in the nuclei of neonatal rat cardiomyocytes at early stages of culture (up to 2 days after plating; not shown).

Transient overexpression of telethonin in U2OS cells led to a strong downregulation of endogenous p53 (Figure 5B, lane 2 versus lane 4). These effects were not observed in the presence of nutlin-3, a compound preventing the interaction between p53 and MDM2, suggesting that MDM2 is required for the effects of telethonin on p53 degradation. Accordingly, expression of classical p53-responsive genes, p21 and MDM2, were suppressed owing to the diminished p53 levels. This prompted us to investigate the underlying molecular mechanism in more detail, and we found direct interaction of telethonin and MDM2 by coimmunoprecipitation assays (Online Figure IX), supporting earlier observations by Tian and coworkers.15 In addition, a direct interaction of p53 and telethonin was detectable by coimmunoprecipitation experiments (Figure 5C) as well as pull-down assays (Figure 5D). Native and SDS-PAGE gel electrophoresis indicated the formation of a high-molecular weight complex (≈150 kDa) between full-length telethonin (wildtype and E13del) and full-length p53 in vitro (Figure 5D, right panels).

Static light scattering and NMR analysis additionally showed that the interaction involves the p53 DNA-binding domain (p53DBD). Static light scattering indicated a molecular weight of 163 kDa for this complex, suggesting that it might consist of multiple telethonin and p53DBD molecules (Figure 5E). NMR spectroscopy further confirms that the telethonin interaction involves the p53DBD (Figure 5F). NMR chemical shift differences between the free and telethonin-bound p53DBD reveal that telethonin contacts the β -sheet of p53DBD, at a site that is remote from the DNA-binding interface (Figure 5F, Online Figure X). Fluorescence polarization (FP) experiments (Figure 5G) and surface plasmon resonance (SPR, Biacore) experiments (Online Figure X) show that the interaction between telethonin and p53DBD has a low micromolar dissociation constant $(K_D=2.2\pm0.2~\mu mol/L$ and $0.765\pm0.03~\mu mol/L$ for FP and SPR, respectively; Online Figure X). These values are comparable to other protein-protein interactions that have been mapped to p53DBD.45-47 It is interesting to note that the interaction of telethonin with titin (Figure 3G) also preferentially involves the β -sheets of the titin Z1-Z2 domains



Knöll et al

Figure 6. Analysis of the effect of telethonin on p53 in vivo. A, Schematic diagram of the construct used to generate telethonin transgenic animals. An alpha myosin heavy chain promoter was used for myocardium-specific expression of a FLAGtagged mouse telethonin cDNA. Human growth hormone poly A tail has been used to enhance stability of the transcript. MHCtelethonin (Tcap)-F and R primers were used for genotyping. B, Western blot analysis of telethonin and p53 gene expression in telethonin transgenic (TG) versus wildtype littermate control animals (nontransgenic, NTG) 2 weeks after transverse aortic constriction (TAC). Note the decrease in p53 gene expression in telethonin transgenic animals. C, Quantification of p53 protein levels in telethonin transgenic animals. Data are normalized to GAPDH. Note that telethonin overexpression decreases p53 protein levels (open bars: wildtype animals [n=3]; solid bars: telethonin transgenic animals [n=3]; *P<0.05; error bars indicate standard deviation [SD]). D, Quantification of p21 mRNA expression in telethonin transgenic animals. The p21 is an important target gene of p53, and the decrease in p21 mRNA is well in accordance with loss of p53 protein expression (open **bars:** wildtype animals [n=3];, **solid bars:** telethonin transgenic animals [n=3]; *P<0.05; **P<0.01; error bars indicate standard deviation [SD].

forming intermolecular β -strand contacts. Similar interactions might contribute to the stabilization of the telethonin–p53DBD complex.

We performed as well a series of F-actin, α -actinin, telethonin, and p53 colocalization studies and found that p53, in contrast to the Z-disk localization of telethonin, is not clearly detectable under spontaneous conditions, neither in the in vivo setting nor in isolated neonatal rat cardiomyocytes in vitro (Online Figures XI and XII). However, after biomechanical or oxidative stress in vivo, such as TAC (Figure 5), or doxorubicin treatment in vitro and in vivo (Online Figures XIII and XIV), we observed a strong induction of p53 in cardiomyocyte nuclei, which is well in accordance with previously published data on p53.48,49 Moreover, under both stress conditions, telethonin colocalized with p53 in cardiomyocyte nuclei (Online Figures XIII and XIV). However, an even stronger increase in p53 nuclear expression was observed after TAC in telethonin-deficient animals, supporting the results of our previous Western blot anal-

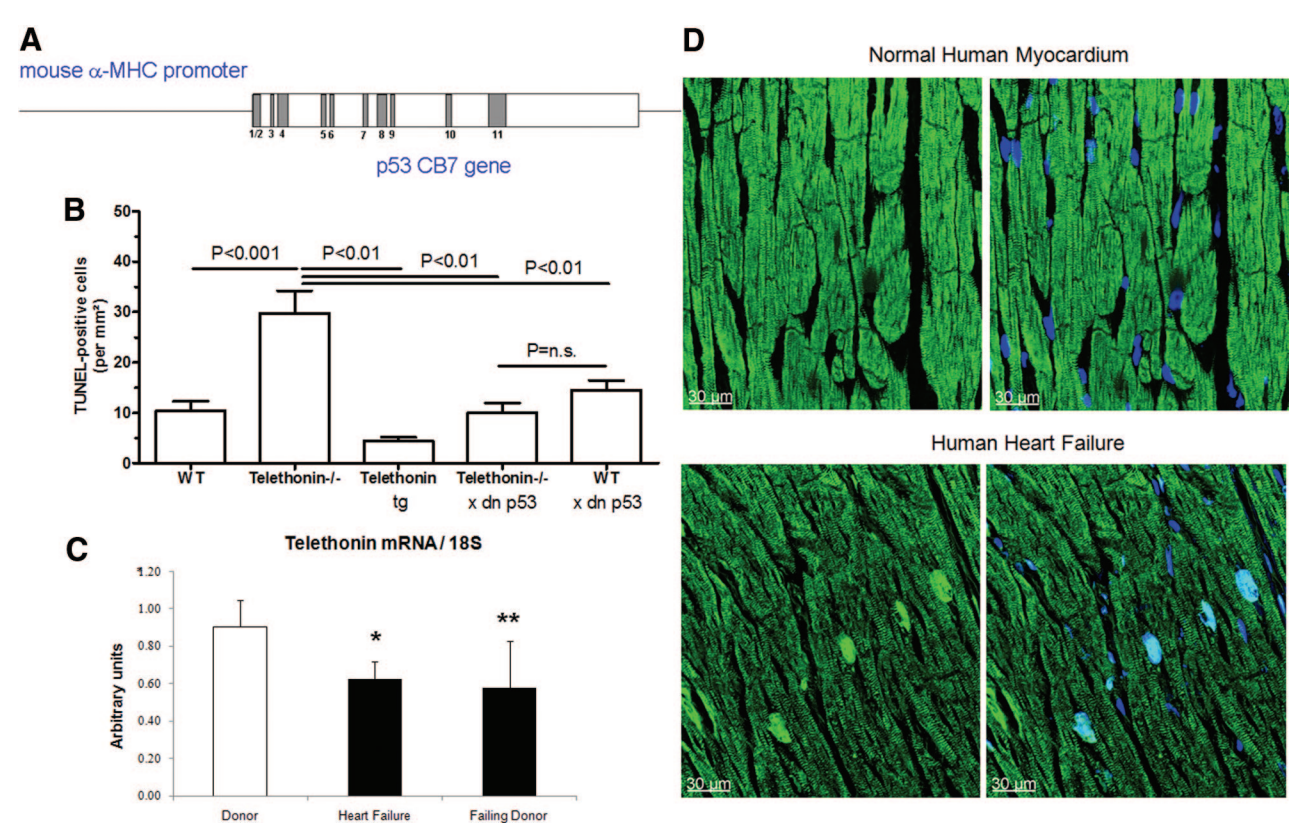


Figure 7. Inhibition of p53 and its effect on telethonin deficiency after TAC and implications for human disease. A, Schematic diagram of the CB7 construct, which encodes the Arg193Pro mutation, a well-known dominant interfering phenotype (ie, dominant negative [dn] p53).⁵¹ These mice have been crossed into the telethonin knockout background resulting in dn p53 / telethonin double transgenic animals. The numbers refer to p53 exons (gray boxes); 1/2 indicates that a fusion was made between exons 1 and 2. **B**, Quantification of apoptosis after transverse aortic constriction (TAC). Note that p53 inhibition in the telethonin knockout background prevents the increase in apoptosis. Wildtype (n=15), telethonin^{-/-} (n=11), telethonin transgenic (n=4), dn p53 (n=13), and dn p53/telethonin double transgenic animals (n=7); error bars indicate standard deviation (SD). **C**, Quantification of telethonin mRNA by quantitative real-time PCR in ventricular myocardium from normal donor organs (n=8), from end-stage heart failure patients taken at the time of transplantation (heart failure n=7), and from failing donor organs with EF <30% (n=9). Data are shown as mean \pm standard deviation (SD). *P<0.05, **P<0.01 versus donors. **D**, Analysis of telethonin localization in human hearts. Note that under physiological (no disease) conditions, telethonin is present at the sarcomeric Z-disk but not in cardiac nuclei (upper panel). In heart failure, telethonin in green).

ysis (Figure 2 and Figure 4). Telethonin/p53 colocalization was also observed when we transfected neonatal rat cardiomyocytes in vitro using a GFP-telethonin construct (Online Figure XV).

On the basis of these data, we assumed that telethonin at least supports MDM2-mediated p53 degradation. As a consequence we aimed to analyze the effects of telethonin overexpression on myocardial function under in vivo conditions and generated telethonin transgenic animals. We used the myocardium-specific alpha myosin heavy chain promoter and a FLAG-tagged mouse telethonin cDNA (Figure 6). Again, to our surprise, these animals did not exhibit any spontaneous phenotype (Online Table II).⁵⁰ Of note, they develop less apoptosis as well as less p53 expression in comparison with wildtype littermate controls after TAC (Figure 6). The decrease in apoptotic (TUNEL positive) cells in telethonin transgenic animals is particularly interesting and might indicate potential protective effects of telethonin overexpression.

We then assumed that p53 determines the negative outcome in telethonin-deficient animals following biomechanical stress, and we used a transgenic line overexpressing a well-characterized dominant negative p53 mutant (ie, the Arg193Pro mutation)^{51,52} to inactivate this protein in the telethonin^{-/-} background (Figure 7A). The dnp53/ telethonin^{-/-} double transgenic animals did not develop any spontaneous phenotype, and they did not exhibit any significant change in myocardial function following TAC. However, genetic inhibition of p53 in the telethonin deficient background significantly inhibited the increase in apoptosis found after biomechanical stress in telethonin^{-/-} animals alone (Figure 7B).

In order to study telethonin mRNA expression in the human heart we analyzed myocardial samples from end-stage heart failure patients and found significant downregulation in comparison with normal donor hearts (Figure 7C), as well as an increase in nuclear telethonin (Figure 7D). This may have implications for p53 expression and p53-related apoptosis, both of which have previously been shown to be elevated in these patients. We also found downregulation of telethonin in acute donor organ failure, suggesting that this effect is not restricted to the setting of chronic end-stage failure.

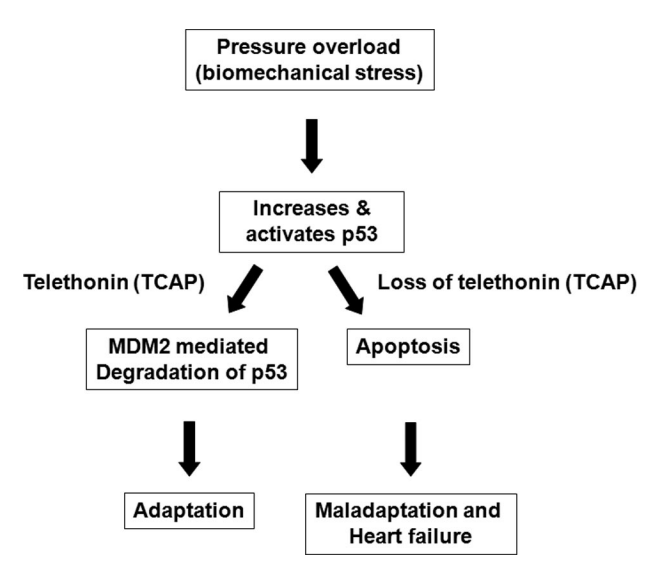


Figure 8. Proposed model depicting telethonin as an essential signaling component in the heart. On the basis of our in vitro and in vivo data, we assume that telethonin binds to p53 as well as to the E3 ubiquitin ligase MDM2, essentially supporting p53 degradation. Loss of or mutations in telethonin, together with an increase in biomechanical stress, causes maladaptation, apoptosis, and global heart failure.

Discussion

Here we demonstrate a model for which a primary defect in an integral Z-disk component is not associated with any cardiac phenotype or functional abnormality under basal conditions.⁵³ However, pressure overload causes a maladaptive response in homozygous telethonin^{-/-} hearts, ultimately leading to global heart failure in vivo. Loss of the p53-ligand telethonin is associated with an increase in p53 as well as elevated apoptosis following an increase in afterload, which is the first description of a Z-disk component to do so. Moreover, by binding to p53's DNA-binding domain, telethonin is potentially able to repress the function of this important transcription factor.

Telethonin, which was shown to be phosphorylated in vitro by the titin kinase,⁷ does not seem to have a function during embryonic development in vivo. A recent study⁵⁴ reported a defect in C2C12 myoblast differentiation when telethonin was downregulated by the use of siRNAs. It remains to be elucidated whether there are differences in vivo and in vitro or whether the telethonin siRNAs per se exhibit off target effects that account for the observed differences. In addition, loss of telethonin in zebrafish or xenopus is associated with a spontaneous defect30,31; as such, it will be important to elucidate in future whether telethonin in mammalian hearts acquired additional functions during evolution, whether sofar-unknown telethonin homologue genes are upregulated, or whether differences in Z-disk structure account for the observed differences. Our data are generally consistent with a recent report whereby telethonin binds in an antiparallel (2:1) sandwich complex to the titin Z1-Z2 domains.4 However, telethonin clearly is not required to stabilize the sarcomere structure. Instead, telethonin may serve as a pivotal element in cardiac signaling by controlling apoptosis and cell death via p53. Our data are compatible with a direct molecular link

between the sarcomeric Z-disk and cardiac performance, as well as gene transcription and cell survival (mechanotranscriptional coupling, or MTC), although additional data need to be provided to entirely support such a functional link. It might well be that Z-disk proteins carry at least 2 different functions: (1) a structural function that might be dismissible, particularly in "peripheral" Z-disk proteins, and (2) a regulatory function, which as in this case, might be much more important. One implication of this could be that cardiomyopathy and associated heart failure, which can be caused by mutations in Z-disk components (now regarded as a "hot spot" for these mutations⁵⁵), might be seen as a disease caused by "defects in cardiac regulation" or of "defects in mechanotranscriptional coupling."

In conclusion, this study might change the previous concept of Z-disk structure, which we now suggest to also be a pivotal node for apoptosis, essentially by linking telethonin to p53 (Figure 8). In contrast to previous views, telethonin is not an indispensable component of the cardiac titin anchoring system, and cardiac-specific telethonin overexpression is not immediately associated with Z-disk pathology and as such is compatible with life. Instead, under normal conditions, actin cross-linking may be sufficient to keep the sarcomere structure viable, despite loss of telethonin. With an increase in hemodynamic load or an increase in biomechanical or oxidative stress, however, telethonin deficiency leads directly to enhanced p53 levels and as such promotes an increase in apoptosis and cell death, thus initiating the development of heart failure, an effect that might be called *mechanoptosis*.

Acknowledgments

Prof. J. Robbins is acknowledged for providing the α MHC promoter. Dr B. North, Department of Biostatistics, Imperial College, London, is gratefully acknowledged for his support with regard to the statistics.

Sources of Funding

Dr R. Knöll is supported by DFG Kn 448/9-1, DFG Kn 448 10-1, Fritz Thyssen Stiftung, British Heart Foundation (PG11/34/28793) and FP7-PEOPLE-2011-IRSES, Proposal No 291834, SarcoSi. Dr W. Linke (Li 690/7-1) and Dr L. Maier (MA 1982/2-2, MA 1982/4-1) are funded by the DFG. Dr G. Faulkner and Dr S. Miocic are supported by grant GGP04088 from the Telethon Foundation—Italy, and Dr Faulkner acknowledges support from the Fondazione Cariparo, Italy (Progetto Eccellenza 2010 CROMUS). Dr H. Granzier acknowledges grant HL062881. Prof. Dr H.C. H. Kessler, Dr P. Zou, Dr F. Hagn, and Prof. M. Sattler acknowledge support by the Elitenetzwerk Bayern and the DFG (SFB594). Prof. M. Wilmanns acknowledges funding from FWF/DFG (P1906). Dr P. Barton is supported by the NIHR Cardiovascular Biomedical Research Unit of Royal Brompton and Harefield NHS Foundation Trust and Imperial College London.

Disclosures

None.

References

 Knöll R, Hoshijima M, Hoffman HM, Person V, Lorenzen-Schmidt I, Bang ML, Hayashi T, Shiga N, Yasukawa H, Schaper W, McKenna W, Yokoyama M, Schork NJ, Omens JH, McCulloch AD, Kimura A, Gregorio CC, Poller W, Schaper J, Schultheiss HP, Chien KR. The cardiac mechanical stretch sensor machinery involves a Z disc complex that is defective in a subset of human dilated cardiomyopathy. *Cell*. 2002; 111:943–955.

- Knöll R, Kostin S, Klede S, Savvatis K, Klinge L, Stehle I, Gunkel S, Kotter S, Babicz K, Sohns M, Miocic S, Didie M, Knoll G, Zimmermann WH, Thelen P, Bickeboller H, Maier LS, Schaper W, Schaper J, Kraft T, Tschope C, Linke WA, Chien KR. A common MLP (muscle LIM protein) variant is associated with cardiomyopathy. Circ Res. 2010;106:695–704.
- 3. Knöll R, Postel R, Wang J, Kratzner R, Hennecke G, Vacaru AM, Vakeel P, Schubert C, Murthy K, Rana BK, Kube D, Knoll G, Schafer K, Hayashi T, Holm T, Kimura A, Schork N, Toliat MR, Nurnberg P, Schultheiss HP, Schaper W, Schaper J, Bos E, Den Hertog J, van Eeden FJ, Peters PJ, Hasenfuss G, Chien KR, Bakkers J. Laminin-alpha4 and integrin-linked kinase mutations cause human cardiomyopathy via simultaneous defects in cardiomyocytes and endothelial cells. Circulation. 2007:116:515–525.
- Zou P, Pinotsis N, Lange S, Song YH, Popov A, Mavridis I, Mayans OM, Gautel M, Wilmanns M. Palindromic assembly of the giant muscle protein titin in the sarcomeric Z-disk. *Nature*. 2006;439:229–233.
- Bertz M, Wilmanns M, Rief M. The titin-telethonin complex is a directed, superstable molecular bond in the muscle Z-disk. *Proc Natl Acad Sci* USA. 2009;106:13307–13310.
- Haworth RS, Cuello F, Herron TJ, Franzen G, Kentish JC, Gautel M, Avkiran M. Protein kinase D is a novel mediator of cardiac troponin I phosphorylation and regulates myofilament function. *Circ Res.* 2004;95: 1091–1099
- Mayans O, van der Ven PF, Wilm M, Mues A, Young P, Furst DO, Wilmanns M, Gautel M. Structural basis for activation of the titin kinase domain during myofibrillogenesis. *Nature*. 1998;395:863–869.
- Miller MK, Granzier H, Ehler E, Gregorio CC. The sensitive giant: the role of titin-based stretch sensing complexes in the heart. *Trends Cell Biol*. 2004;14:119–126.
- Osio A, Tan L, Chen SN, Lombardi R, Nagueh SF, Shete S, Roberts R, Willerson JT, Marian AJ. Myozenin 2 is a novel gene for human hypertrophic cardiomyopathy. *Circ Res*. 2007;100:766–768.
- Kontrogianni-Konstantopoulos A, Bloch RJ. The hydrophilic domain of small ankyrin-1 interacts with the two N-terminal immunoglobulin domains of titin. J Biol Chem. 2003;278:3985–3991.
- Faulkner G, Pallavicini A, Comelli A, Salamon M, Bortoletto G, Ievolella C, Trevisan S, Kojic S, Dalla Vecchia F, Laveder P, Valle G, Lanfranchi G. FATZ, a filamin-, actinin-, and telethonin-binding protein of the Z-disc of skeletal muscle. *J Biol Chem.* 2000;275:41234–41242.
- Frey N, Olson EN. Calsarcin-3, a novel skeletal muscle-specific member of the calsarcin family, interacts with multiple Z-disc proteins. *J Biol Chem.* 2002;277:13998–14004.
- Furukawa T, Ono Y, Tsuchiya H, Katayama Y, Bang M, Labeit D, Labeit S, Inagaki N, Gregorio C. Specific interaction of the potassium channel beta-subunit minK with the sarcomeric protein T-cap suggests a T-tubulemyofibril linking system. *J Mol Biol*. 2001;313:775–784.
- Kojic S, Medeot E, Guccione E, Krmac H, Zara I, Martinelli V, Valle G, Faulkner G. The Ankrd2 protein, a link between the sarcomere and the nucleus in skeletal muscle. *J Mol Biol.* 2004;339:313–325.
- Tian LF, Li HY, Jin BF, Pan X, Man JH, Zhang PJ, Li WH, Liang B, Liu H, Zhao J, Gong WL, Zhou T, Zhang XM. MDM2 interacts with and downregulates a sarcomeric protein, TCAP. *Biochem Biophys Res Commun.* 2006;345:355–361.
- Witt SH, Granzier H, Witt CC, Labeit S. MURF-1 and MURF-2 target a specific subset of myofibrillar proteins redundantly: towards understanding MURF-dependent muscle ubiquitination. *J Mol Biol*. 2005;350: 713–722.
- Mihatsch K, Nestler M, Saluz HP, Henke A, Munder T. Proapoptotic protein Siva binds to the muscle protein telethonin in cardiomyocytes during coxsackieviral infection. *Cardiovasc Res.* 2009;81:108–115.
- Ferreiro A, Mezmezian M, Olive M, Herlicoviez D, Fardeau M, Richard P, Romero NB. Telethonin-deficiency initially presenting as a congenital muscular dystrophy. *Neuromuscul Disord*. 2011;21:433–438.
- Moreira ES, Wiltshire TJ, Faulkner G, Nilforoushan A, Vainzof M, Suzuki OT, Valle G, Reeves R, Zatz M, Passos-Bueno MR, Jenne DE. Limb-girdle muscular dystrophy type 2G is caused by mutations in the gene encoding the sarcomeric protein telethonin. *Nat Genet*. 2000;24: 163–166.
- Olive M, Shatunov A, Gonzalez L, Carmona O, Moreno D, Quereda LG, Martinez-Matos JA, Goldfarb LG, Ferrer I. Transcription-terminating mutation in telethonin causing autosomal recessive muscular dystrophy type 2G in a European patient. *Neuromuscul Disord*. 2008;18:929–933.
- Bos JM, Poley RN, Ny M, Tester DJ, Xu X, Vatta M, Towbin JA, Gersh BJ, Ommen SR, Ackerman MJ. Genotype–phenotype relationships

- involving hypertrophic cardiomyopathy-associated mutations in titin, muscle LIM protein, and telethonin. *Mol Genet Metab.* 2006;88:78-85.
- Hayashi T, Arimura T, Itoh-Satoh M, Ueda K, Hohda S, Inagaki N, Takahashi M, Hori H, Yasunami M, Koga Y, Nakamura H, Matsuzaki M, Choi BY, Bae SW, Park JE, Knöll R, Hoshijima M, Chien KR, Kimura A. TCAP mutations in hypertrophic cardiomyopathy and dilated cardiomyopathy. *J Am Coll Cardiol*. 2004;44:2192–2201.
- Mazzone A, Strege PR, Tester DJ, Bernard CE, Faulkner G, Degiorgio R, Makielski JC, Stanghellini V, Gibbons SJ, Ackerman MJ, Farrugia G. A mutation in telethonin alters Nav1.5 function. *J Biol Chem.* 2008;283: 16537–16544.
- 24. Marziliano N, Pilotto A, Grasso M, Pasotti M, Arbustini E. Deletion of Glu at codon 13 of the TCAP gene encoding the titin-cap-telethonin is a rare polymorphism in a large Italian population. *Mol Genet Metab*. 2006;89:286–287.
- Perrot A, Posch MG, Osterziel KJ. Deletion of Glu at codon 13 in the TCAP gene encoding the Z-disc protein titin-cap/telethonin is a rare non-synonymous polymorphism. *Mol Genet Metab*. 2006;88:199–200.
- Opitz CA, Kulke M, Leake MC, Neagoe C, Hinssen H, Hajjar RJ, Linke WA. Damped elastic recoil of the titin spring in myofibrils of human myocardium. *Proc Natl Acad Sci U S A*. 2003;100:12688–12693.
- Zou P, Gautel M, Geerlof A, Wilmanns M, Koch MH, Svergun DI. Solution scattering suggests cross-linking function of telethonin in the complex with titin. J Biol Chem. 2003;278:2636–2644.
- Sanger JW, Wang J, Holloway B, Du A, Sanger JM. Myofibrillogenesis in skeletal muscle cells in zebrafish. *Cell Motil Cytoskeleton*. 2009;66: 556–566
- Wang J, Shaner N, Mittal B, Zhou Q, Chen J, Sanger JM, Sanger JW. Dynamics of Z-band based proteins in developing skeletal muscle cells. *Cell Motil Cytoskeleton*. 2005;61:34–48.
- Sadikot T, Hammond CR, Ferrari MB. Distinct roles for telethonin N-versus C-terminus in sarcomere assembly and maintenance. *Dev Dyn.* 2010;239:1124–1135.
- Zhang R, Yang J, Zhu J, Xu X. Depletion of zebrafish Tcap leads to muscular dystrophy via disrupting sarcomere-membrane interaction, not sarcomere assembly. *Hum Mol Genet*. 2009;18:4130–4140.
- Markert CD, Meaney MP, Voelker KA, Grange RW, Dalley HW, Cann JK, Ahmed M, Bishwokarma B, Walker SJ, Yu SX, Brown M, Lawlor MW, Beggs AH, Childers MK. Functional muscle analysis of the Tcap knockout mouse. *Hum Mol Genet*. 2010;19:2268–2283.
- Crow MT, Long X, Guglielmi MB, Asai T, Lakatta EG. The role of the tumor suppressor gene p53 in cardiomyocyte apoptosis. *Heart Failure Reviews*. 1998;3:45–61.
- Crow MT. Revisiting p53 and its effectors in ischemic heart injury. CardiovascRes. 2006;70:401–403.
- George I, Bish LT, Kamalakkannan G, Petrilli CM, Oz MC, Naka Y, Sweeney HL, Maybaum S. Myostatin activation in patients with advanced heart failure and after mechanical unloading. Eur J Heart Fail. 2010;12:444–453.
- Heineke J, Auger-Messier M, Xu J, Sargent M, York A, Welle S, Molkentin JD. Genetic deletion of myostatin from the heart prevents skeletal muscle atrophy in heart failure. *Circulation*. 2010;121:419–425.
- Reisz-Porszasz S, Bhasin S, Artaza JN, Shen R, Sinha-Hikim I, Hogue A, Fielder TJ, Gonzalez-Cadavid NF. Lower skeletal muscle mass in male transgenic mice with muscle-specific overexpression of myostatin. Am J Physiol Endocrinol Metab. 2003;285:E876–E888.
- Rodgers BD, Interlichia JP, Garikipati DK, Mamidi R, Chandra M, Nelson OL, Murry CE, Santana LF. Myostatin represses physiological hypertrophy of the heart and excitation–contraction coupling. *J Physiol*. 2009:587:4873–4886.
- Bish LT, Morine KJ, Sleeper MM, Sweeney HL. Myostatin is upregulated following stress in an Erk-dependent manner and negatively regulates cardiomyocyte growth in culture and in a mouse model. *PLoS One*. 2010;5:e10230.
- Sharma M, Kambadur R, Matthews KG, Somers WG, Devlin GP, Conaglen JV, Fowke PJ, Bass JJ. Myostatin, a transforming growth factor-beta superfamily member, is expressed in heart muscle and is upregulated in cardiomyocytes after infarct. *J Cell Physiol*. 1999;180:1–9.
- Wang BW, Chang H, Kuan P, Shyu KG. Angiotensin II activates myostatin expression in cultured rat neonatal cardiomyocytes via p38 MAP kinase and myocyte enhance factor 2 pathway. *J Endocrinol*. 2008;197:85–93.
- Morissette MR, Stricker JC, Rosenberg MA, Buranasombati C, Levitan EB, Mittleman MA, Rosenzweig A. Effects of myostatin deletion in aging mice. *Aging Cell*. 2009;8:573–583.

- 43. Nicholas G, Thomas M, Langley B, Somers W, Patel K, Kemp CF, Sharma M, Kambadur R. Titin-cap associates with, and regulates secretion of, Myostatin. J Cell Physiol. 2002;193:120-131.
- 44. Yi X, Bekeredjian R, DeFilippis NJ, Siddiquee Z, Fernandez E, Shohet RV. Transcriptional analysis of doxorubicin-induced cardiotoxicity. Am J Physiol Heart Circ Physiol. 2006;290:H1098-H1102.
- 45. Hagn F, Klein C, Demmer O, Marchenko N, Vaseva A, Moll UM, Kessler H. BclxL changes conformation upon binding to wild-type but not mutant p53 DNA binding domain. J Biol Chem. 2010;285:3439-3450.
- 46. Muller L, Schaupp A, Walerych D, Wegele H, Buchner J. Hsp90 regulates the activity of wild type p53 under physiological and elevated temperatures. J Biol Chem. 2004;279:48846-48854.
- 47. Tidow H, Veprintsev DB, Freund SM, Fersht AR. Effects of oncogenic mutations and DNA response elements on the binding of p53 to p53binding protein 2 (53BP2). J Biol Chem. 2006;281:32526-32533.
- 48. Nithipongvanitch R, Ittarat W, Cole MP, Tangpong J, Clair DK, Oberley TD. Mitochondrial and nuclear p53 localization in cardiomyocytes: redox modulation by doxorubicin (Adriamycin)? Antioxid Redox Signal. 2007; 9:1001-1008.
- 49. Pikkarainen S, Kennedy RA, Marshall AK, Tham el L, Lay K, Kriz TA, Handa BS, Clerk A, Sugden PH. Regulation of expression of the rat orthologue of mouse double minute 2 (MDM2) by H(2)O(2)-induced oxidative stress in neonatal rat cardiac myocytes. J Biol Chem. 2009;284: 27195-27210.

- 50. Gregorio CC, Trombitas K, Centner T, Kolmerer B, Stier G, Kunke K, Suzuki K, Obermayr F, Herrmann B, Granzier H, Sorimachi H, Labeit S. The NH2 terminus of titin spans the Z-disc: its interaction with a novel 19-kD ligand (T-cap) is required for sarcomeric integrity. J Cell Biol. 1998;143:1013-1027.
- 51. Nakajima H, Nakajima HO, Tsai SC, Field LJ. Expression of mutant p193 and p53 permits cardiomyocyte cell cycle reentry after myocardial infarction in transgenic mice. Circ Res. 2004;94:1606-1614.
- 52. Zhu W, Soonpaa MH, Chen H, Shen W, Payne RM, Liechty EA, Caldwell RL, Shou W, Field LJ. Acute doxorubicin cardiotoxicity is associated with p53-induced inhibition of the mammalian target of rapamycin pathway. Circulation. 2009;119:99-106.
- 53. Frey N, Barrientos T, Shelton JM, Frank D, Rutten H, Gehring D, Kuhn C, Lutz M, Rothermel B, Bassel-Duby R, Richardson JA, Katus HA, Hill JA, Olson EN. Mice lacking calsarcin-1 are sensitized to calcineurin signaling and show accelerated cardiomyopathy in response to pathological biomechanical stress. Nat Med. 2004;10:1336-1343.
- 54. Markert CD, Ning J, Staley JT, Heinzke L, Childers CK, Ferreira JA, Brown M, Stoker A, Okamura C, Childers MK. TCAP knockdown by RNA interference inhibits myoblast differentiation in cultured skeletal muscle cells. Neuromuscul Disord. 2008;18:413-422.
- 55. Bos JM, Ackerman MJ. Z-disc genes in hypertrophic cardiomyopathy: stretching the cardiomyopathies? J Am Coll Cardiol. 2010;55:1136-1138.

Novelty and Significance

What Is Known?

- Telethonin is a small (19 kDa) muscle-specific protein.
- Telethonin is localized to the sarcomeric Z-disk where it interacts with the giant protein titin.
- · Telethonin mutations are associated with various diseases such as limb girdle muscular dystrophy 2 G (LGMD 2G), cardiomyopathy, and intestinal pseudoobstruction.

What New Information Does This Article Contribute?

- · Telethonin deficiency is not associated with a spontaneous phenotype, at least not in the mammalian heart.
- Telethonin is not essential for the mechanical stability of the Z-disk.
- Telethonin promotes cardiac myocyte survival by suppressing p53 mediated apoptosis.

Telethonin mutations are associated with several diseases, but the underlying molecular mechanisms remain not well understood. To analyze the in vivo function of telethonin, we generated genetically altered mouse models and found that telethonin is a dispensable component of the sarcomeric Z-disk. Deletion or cardiac-specific overexpression of telethonin was not associated with a spontaneous cardiac phenotype. However, our results showed that telethonin modulates the turnover of the proapoptotic protein p53 after biomechanical stress. This novel finding links telethonin directly to apoptosis ("mechanoptosis"), which is considered a new cell death associated pathway. We also observed a reduction in the expression of telethonin and an increase in its nuclear abundance in myocardial samples from end-stage heart failure patients, indicating that changes in telethonin may contribute to cardiac maladaptation. These findings suggest that telethonin, together with other Z-diskassociated proteins, might have novel functions in antiapoptotic cell survival pathways.

1	Supplement Material
2	
3	
4	Telethonin deficiency is associated with maladaptation to biomechanical stress in the
5	mammalian heart
6 7	Knöll et al., short title: Telethonin deficiency
8	
9	Ralph Knöll MD, PhD ^{1,14,15,16} ; Wolfgang A. Linke PhD ² , Peijian Zou PhD ^{5,11,12a} , Snježana Miočić MD ⁴ ,
10	Sawa Kostin ¹⁶ , Ching-Hsin Ku ¹⁵ , Stefan Neef MD ¹ , Monika Bug ³ , Katrin Schäfer MD ⁸ , Gudrun Knöll ¹⁵ ,
11	Leanne E Felkin ¹⁷ , Johannes Wessels ¹ , Karl Toischer MD ⁸ , Franz Hagn PhD ^{12a,12b} , Horst Kessler
12	PhD ^{12a,12b} , Michael Didié MD ⁶ , Byambajav Buyandelger PhD ¹ , Thomas Quentin PhD ⁷ , Lars Maier
13	MD ¹ , Nils Teucher MD ¹ , Bernhard Unsöld MD ¹ , Albrecht Schmidt MD ¹ , Emma J Birks ¹⁷ , Sylvia Gunkel
14	PhD1, Patrick Lang PhD9, Henk Granzier PhD10, Wolfram-Hubertus Zimmermann MD6, Loren J. Field
15	PhD8, Georgine Faulkner PhD4, Matthias Dobbelstein MD3, Paul JR Barton 17, 18, Michael Sattler
16	PhD ^{11,12a} , Matthias Wilmanns PhD ⁵ , Kenneth R. Chien MD, PhD ¹³

Materials and Methods

2 Generation of telethonin deficient animals and transverse aortic constriction (TAC) 3 and echocardiography

- Telethonin deficient animals were generated by replacing the coding regions of exon 1 and 2 4
- by a lacZ-neomycin cassette to monitor endogenous gene expression using homologous 5
- recombination (fig. 1). Telethonin transgenic overexpressing animals were generated by 6
- 7 using the alpha myosin heavy chain promoter and a flag tagged mouse cDNA followed by
- the human growth hormone poly A tail (fig. 4 h). dn p53 / telethonin double transgenic 8
- animals were generated by crossing the CB7 line into the telethonin deficient background. 9
- 10 Surgery was carried out using a modified minimally invasive approach as previously
- described¹. Northern, Southern and Western blot analysis was performed as previously 11
- described². 12

1

- Mice were anesthetized with Avertin^R (125 mg/kg, IP) or isoflurane and echocardiography was performed as described previously³. Briefly, transthoracic echocardiography was 13
- 14
- performed by an examiner blinded to the genotype of the animals using a Vevo2100 15
- (VisualSonics, Toronto, Canada) system with a 30 MHz centre frequency transducer. Two-16
- dimensional cine loops with frame rates of >200 frames/s of a long axis view and a short axis 17
- 18 view at mid-level of the papillary muscles as well as M-mode loops of the short axis view
- 19 were recorded.

20

21

35

Cell culture experiments and silencing of telethonin

- Osteosarcoma U2OS cells were transiently transfected with myc-telethonin and 12 hours 22
- later treated for 24 hours with nutlin-3 (8µM final concentration). Cell lysates were analyzed 23
- 24 by SDS-PAGE and Western blotting using the following antibodies: p53 DO-1 (Santa Cruz),
- p21WAF1 EA10 (Calbiochem), Mdm2 2A9 and 2A10, myc 4A6 (Upstate) and actin AC15 25
- 26 (Abcam).
- Neonatal rat cardiomyocytes were grown in F12 medium supplemented with 10% FCS and 27
- PB12 (penicillin G+vitamin B12, Sigma) for 24 hours. The medium was changed and the 28
- 29 cells were transfected with 50nM negative control siRNA and siRNA Telethonin (Darmacon)
- in the presence of 10% FCS. After 48h of silencing, cells were incubated with doxorubicin 30
- (1µM, Sigma) for 12 hours. Cells were treated with MG132 two hours before harvesting. 31
- Whole cell extracts were used for western blot analysis and the membrane was probed with 32
- 33 mouse polyclonal telethonin (1:400) and rabbit polyclonal p53 antibodies (1:200, Santa
- Cruz). Data were normalized to GAPDH (1:10000, Santa.Cruz). 34

RNA extraction, qRT-PCR analysis, RT² Profiler Apoptosis PCR Arrays 36

- 37 RNA from left ventricles was extracted using the RNeasy Fibrous Tissue Mini Kit (Qiagen
- GmbH, Hilden, Germany). 38
- For single quantitative PCR (qRT-PCR): reverse-transcription was performed from 500 ng 39
- 40 total RNA using the iScript cDNA Synthesis Kit (Bio-Rad) according to the manufacturer's
- instructions. PCR was performed in duplicate using the Bio-Rad iCycler (Bio-Rad) and SYBR 41
- 42 Green as fluorescence. Primer sequences are available upon request.
- 43 For the SA Biosciences apoptosis gene expression array: RNA quantity and quality was
- assayed by the NanoDrop spectrometer and 1µg of the RNA was used for the cDNA 44
- 45 synthesis with the reagents and primers provided (according to the manufacturer's protocol,
- SABiosciences). Gene expression of 84 key apoptosis genes was profiled by gRT-PCR 46

- based RT² Profiler Apoptosis PCR Arrays (mouse: PAMM-012) using the RT² SYBR
- 2 Green/Rox Master mix. gRT-PCRs were performed in 96-well plate format using the ABI
- 3 7900 Fast Real-Time PCR System (Applied Biosystems). All data were analysed by RT²
- 4 Profiler Web-Based PCR Array Data Analysis (SABiosciences).

5

- 7 Electrophysiology, electrocardiograms (ECG), isolation of cardiac myocytes, 8 intracellular Ca²⁺ transients and myocyte shortening
- 9 All studies were done under blind conditions. After obtaining surface-ECG recordings from
- adult (26-38 week) WT (n=7) and telethonin-KO (n=8) mice during mild anaesthesia, hearts
- were explanted and single myocytes isolated as reported previously⁴⁻⁵. Ca²⁺ transients were
- recorded using Fluo-3 AM, SR load and NCX function estimated by caffeine application.
- 13 Patch clamp electrophysiology (voltage clamp) was used to record stimulated action
- 14 potentials.

15

16

Sarcomere stretch and titin localization

- Myofibrils were prepared from telethonin-deficient or wildtype tissue as described previously⁶.
- Under a Zeiss Axiovert-135 inverted microscope, single myofibrils were attached to the tip of
- 19 two micromanipulator-controlled glass microneedles, and were stretched in relaxing solution⁶
- to different SLs, before they were stained using anti-Z1Z2 titin antibody (a kind gift of Prof. S.
- Labeit, Mannheim) and FITC-conjugated secondary antibody ⁷. Some cardiac myofibrils were
- exposed to 0.3 mg/ml Ca²⁺-independent gelsolin-fragment for 5 min to remove actin filaments
- 23 (complete actin removal was confirmed by rhodamine-phalloidin staining)⁶. The width of the
- 24 fluorescence signal was evaluated using ImageJ software by calculating the full-width at half-
- 25 maximum (FWHM) signal in intensity profiles along the myofibril axis.

26

27

In vitro protein interaction assay

- 28 Z1Z2 titin, MLP, telethonin as well as its mutants were expressed and purified as previously
- described⁸. Z1Z2-telethonin complexes were formed and analyzed on native gels and gel filtration columns as previously described⁸⁻⁹. The molecular masses during gel filtration
- 30 filtration columns as previously described. The molecular masses during gel filtration chromatography were measured by a static light scattering detector (Malvern, GPC5130).

32 33

Pull-down assay

- 34 Equal amount of recombinant His6-Z-tag, His-Z-tag-telethonin and His-Z-tag-telethonin
- 35 E13del mutant in the buffer of 20 mM Tris/HCl, pH 8.0, 1 mM TCEP, 5mM imidazole and 300
- 36 mM NaCl were loaded onto Ni-NTA columns (1mL) respectively. After washing with 20 x bed
- 37 volumes of the buffer, p53 in the same buffer was loaded onto the column. The bound
- proteins were eluted with 300 mM imidazole in the buffer and analyzed by 12% SDS-PAGE,
- transferred to nitrocellulose, and probed with rabbit polyclonal p53 antibodies.

40 41

Preparation of telethonin, p53DBD and the telethonin-p53DBD complex

- 42 Full-length wild type (residues 1-167) or E13del telethonin as well as wild type and various
- 43 E13 mutants of telethonin (residues 1-90) (see Fig 2c) were prepared under denaturing
- condition as described previously⁸. The protein eluated from the Ni-NTA column was further
- 45 purified on a Superdex 75 (16 x 60) column that was pre-equilibrated with 20 mM Hepes, pH

7.2, 100 mM NaCl, 1 mM TCEP, 1 M urea. p53 DNA binding domain (DBD, residues 94-312) was prepared as described previously 10 . The complex was formed by dropping a solution of telethonin (full-length) into a 50 μ M solution of p53DBD up to a two-fold molar excess of telethonin. The final concentration of urea should be controlled to be below 0.5 M. The complex solution was concentrated. Buffer exchange to 20 mM Hepes, pH 7.2, 100 mM NaCl, 1 mM TCEP and further purification was done by gel filtration using a Superdex 75 (16 x 60) column, pre-equilibrated with the same buffer.

Fluorescence polarization

Fluorescein labelling of p53DBD was achieved by mixing equimolar amounts (200μM) of p53DBD and 5-(and-6)-carboxyfluorescein succinimidyl ester (Invitrogen) in 20 mM sodium phosphate pH7.0, 100 mM sodium chloride, 1 mM TCEP. After incubation for 1h at 10°C, the reaction was quenched by the addition of a ten-fold molar excess of Tris buffer pH7.5. Separation of the labelled protein from the free label was done by passage over a Superdex-75 gel filtration column. Labelling degree was between 30 and 60%. Fluorescence polarization experiments were performed at room temperature with a BMG Polarstar multimode plate reader (BMG Labtec, Offenburg, Germany) using 0.5 μM fluorescein-labelled p53DBD in 10 mM sodium phosphate pH7.2, 1 mM TCEP and titrating in increasing amounts of full-length telethonin (residues 1-167). Three individual measurements were done for error estimation. Fitting of the obtained binding curve was done using a one-site binding model.

NMR spectroscopy

U-²H,¹⁵N-labelled p53DBD for NMR studies was prepared using M9-medium supplemented with 1g/l ¹⁵NH₄Cl, 2g/l ²H,¹³C glucose in 99.9% D₂O (Eurisotop, Saarbrücken, Germany).
 Nuclear magnetic resonance (NMR) experiments were done at 293K on a Bruker Avance900 spectrometer (Bruker Biospin, Rheinstetten, Germany).

For probing the p53DBD-telethonin interaction, 1H , ^{15}N TROSY or 1H , ^{15}N CRINEPT-HMQC experiments were recorded with a complex consisting of 50 μ M U- 2H , ^{15}N p53DBD and unlabelled full-length telethonin in 20 mM sodium phosphate pH7.2, 100 mM sodium chloride, 1 mM TCEP and 5% (v/v) D₂O. 192 transients per increment and 140 increments in the indirect ^{15}N dimension were recorded resulting in a total measuring time of 8h for each experiment.

Apoptosis

Apoptosis was analyzed using the "Apoptag peroxidase *in situ* apoptosis detection kit" (Millipore – Chemicon, MA, USA) as well as the "Roche - In Situ Cell Death Detection Kit, (Roche, #116847959110) according to the manufacturer's instructions. We used 7 wildtype sham, 15 wildtype transverse aortic constriction (TAC), 7 telethonin-knockout sham, 11 telethonin-knockout TAC, 4 telethonin transgenic TAC, 7 telethonin-knockout / dn p53 double transgenic TAC and 13 dn p53 TAC animals. 4 different microscope fields per animal were examined, results were averaged per mouse and expressed as apoptotic cells per mm² (with one microscope field corresponding to 0.045 mm²).

Immunoprecipitation

For immunoprecipation of telethonin with p53 and MDM2 full length as well as amino- and carboxy-terminal human telethonin cDNAs were cloned into pcDNA3-HA (a modified pcDNA3.1 vector (Invitrogen) with an HA tag (YPYDVPDYA). All constructs were verified by sequencing.

Human osteosarcoma cells (U2OS) were grown in Dulbecco's modified Eagle's medium (DMEM) supplemented with 10% fetal bovine serum. Cells were transiently transfected with telethonin in the presence of Nutlin (8µM, Calbiochem; 24 hours). The cell lysates were immunoprecipitated using the Mammalian HA tag Co-IP kit (Pierce) according to the manufacturer's protocol, with anti-HA antibody-coupled agarose beads (10µg) and U2OS cell lysate (600µg). The protein complexes were resolved by SDS-PAGE, blotted and probed with the anti-p53 monoclonal antibody DO-1 (Santa Cruz). The bound p53 was identified by chemiluminescence (ECL plus, Amersham) using the HRP coupled anti-mouse antibody (Sigma). To study the interaction of MDM2 with telethonin U2OS cells transfected with the full-length T-cap (Tel-FL), T-cap N-terminus (Tel-N) and T-cap C-terminus (Tel-C) and/or with the empty plasmid in the presence of MG132 (0.2µM). The co-immunoprecipitation were performed by incubating anti-MDM2 (2A10) with cell lysate for 1.5h , then protein A-Sepharose (Amersham Pharmacia) was added and lysates were incubated at +4°C for 2h. Protein-antibody complexes were separated by SDS-PAGE, blotted and probed with mouse polyclonal anti T-cap antibody.

Immunolabeling and fluorescent microscopy

For the co-localization study in neonatal rat cardiomyocytes cells were treated with doxorubicin (1µM, Sigma) for 24 hours, fixed and incubated with rat polyclonal anti-telethonin antibody (kindly provided by Prof. Georgine Faulkner) rabbit polyclonal anti-p53 (FL 393, Santa Cruz), and/or mouse monoclonal p53 (1C12, Cell signalling), mouse monoclonal anti-alpha actinin (Sigma) and phalloidin conjugated Alexa 350 antibody. The secondary antibodies used were Alexa-labeled 633 anti-rat, Alexa- labelled 488 anti-rabbit and Alexa-labelled 488 anti-mouse (Invitrogen) antibody.

For the co-localization study in animals, hearts were mounted in tissue Tec and cryosections 5 mm thick were prepared. Cryosections were air dried and fixed for 10 min in acetone (-20°C). After washing in phosphate buffered saline (PBS) sections were incubated with 1% bovine serum albumin for 30 minutes to block non-specific binding sites. After rinsing in PBS, the samples were incubated overnight with the following antibodies: primarily labeled anti-p53 with Alexa Fluor® 488 (FL 393, Santa Cruz), primary monoclonal antibodies against alpha-actinin (clone EA-53, Sigma) or polyclonal antibodies against telethonin (polyclonal anti-telethonin antibody provided by Prof. Georgine Faulkner). After incubation with the primary antibodies, the sections were thoroughly washed in PBS and incubated with secondary Alexa Fluor® 488- Alexa Fluor® 555-conjugated anti-mouse or anti-rabbit IgG (Molecular Probes). F-actin was labeled with phalloidin conjugated with Fluor® 633 (Sigma) and nuclei were stained with DAPI (Molecular Probes).

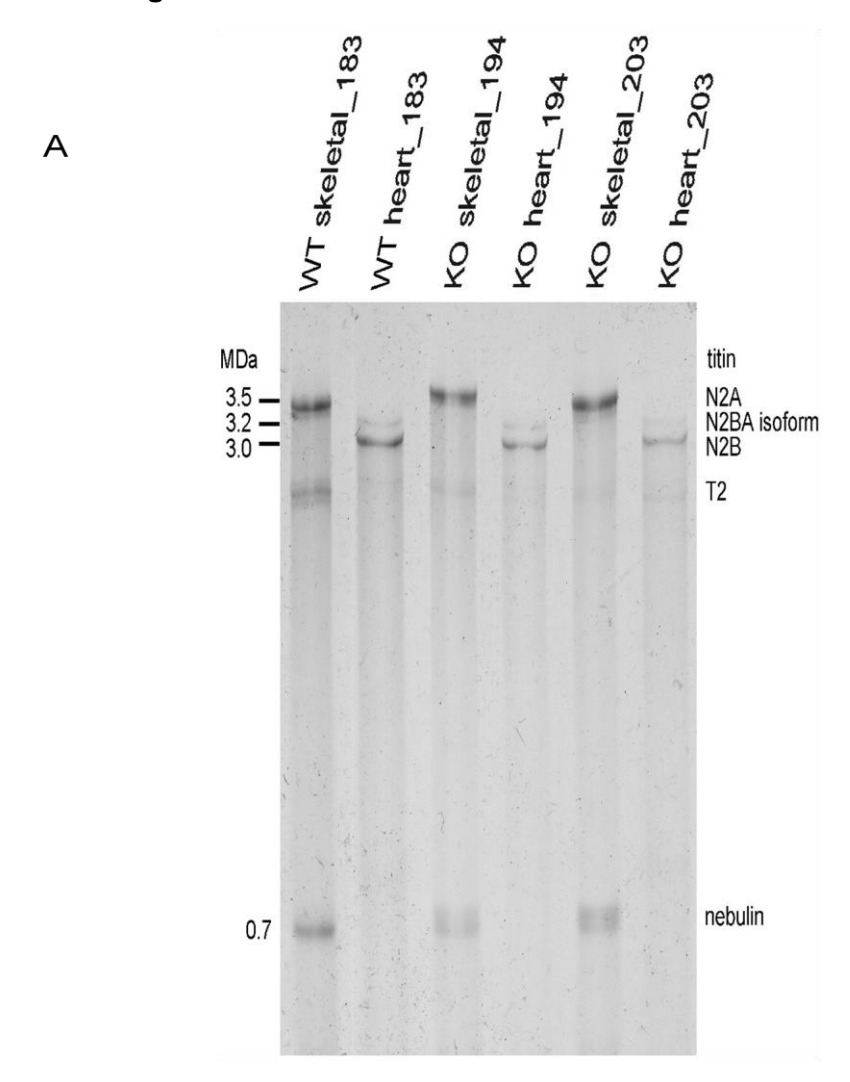
Tissue sections were examined by laser scanning confocal microscopy (Leica TCS SP2). Series of confocal optical sections were taken using a Leica Planapo x40/1.00 or x63/1.32 objective lens. Each recorded image was taken using dual-channel scanning and consisted of 1024 x 1024 pixels. To improve image quality and to obtain a high signal to noise ratio, each image from the series was signal-averaged. After data acquisition, the images were transferred to a Silicon Graphics workstation (Silicon Graphics) for restoration and three-dimensional reconstruction using Imaris 4.5 multichannel image processing software (Bitplane, Zürich, Switzerland).

Quantitative immunofluorescence measurements

In brief, cryosections from at least two different levels in each mouse were used. All samples were immunolabeled simultaneously with identical conditions of fixation and dilutions of primary and secondary antibodies. Sections exposed to PBS instead of primary antibodies served as negative controls. For each heart at least 10 random fields of vision were analyzed with confocal microscopy. Immunolabeled cryosections were studied using image analysis (Leica) and Image J software. Quantification of p53 was performed blinded to the type of

section having on the screen only one channel showing DAPI labeling. For each quantification a specific setting was established and kept constant in all measurements. Quantification of p53 was performed by measurements of fluorescence intensity by using a range of 0 to 255 gray values. Arbitrary units of the fluorescence intensity were calculated per unit nuclear area (AU/µm2).

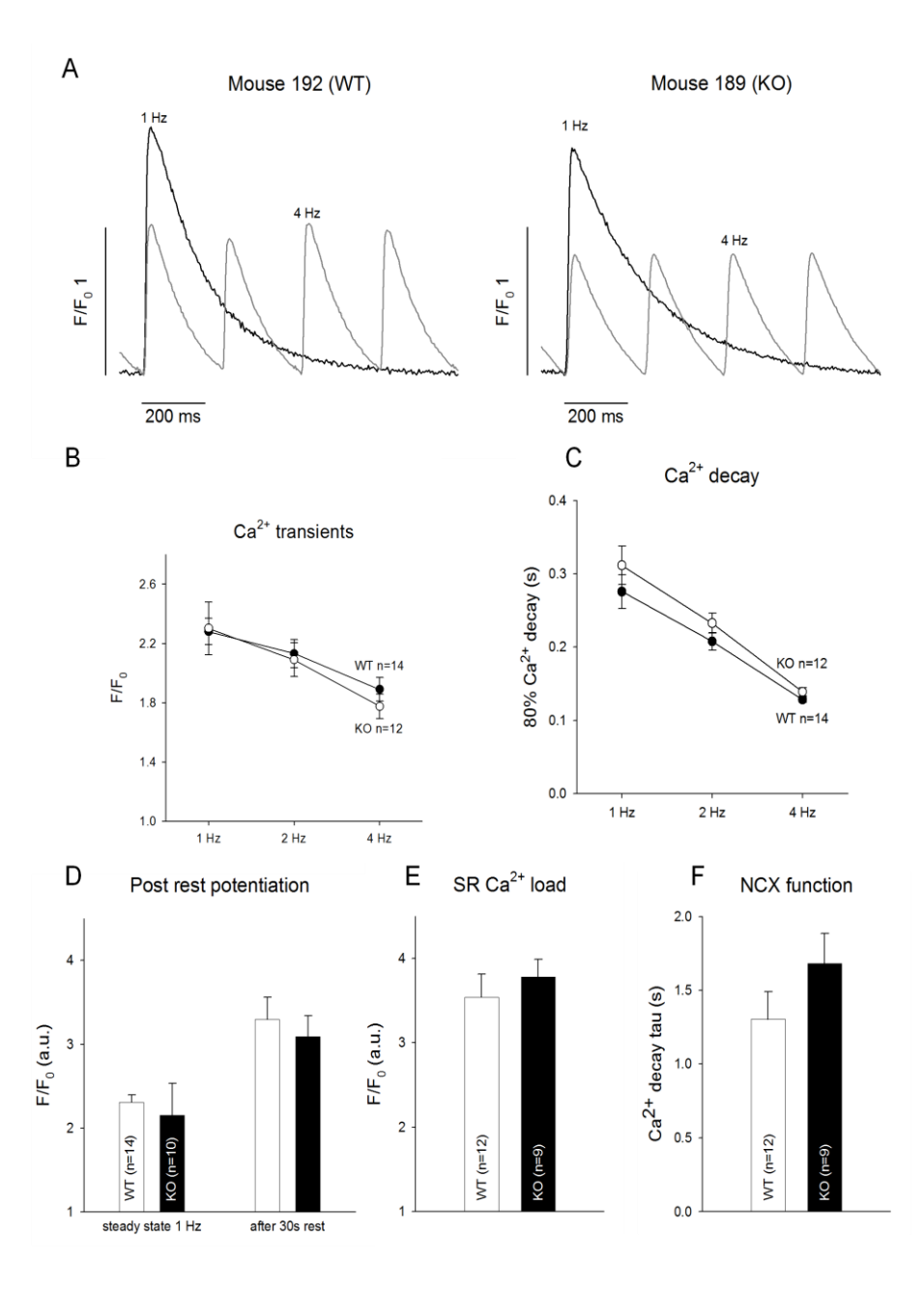
Online Figure I



9 Online Figure I: No change in titin expression between wildtype and homozygous telethonin 10 knockout animals has been observed, neither in cardiac nor in skeletal muscle.

1 Online Figure II



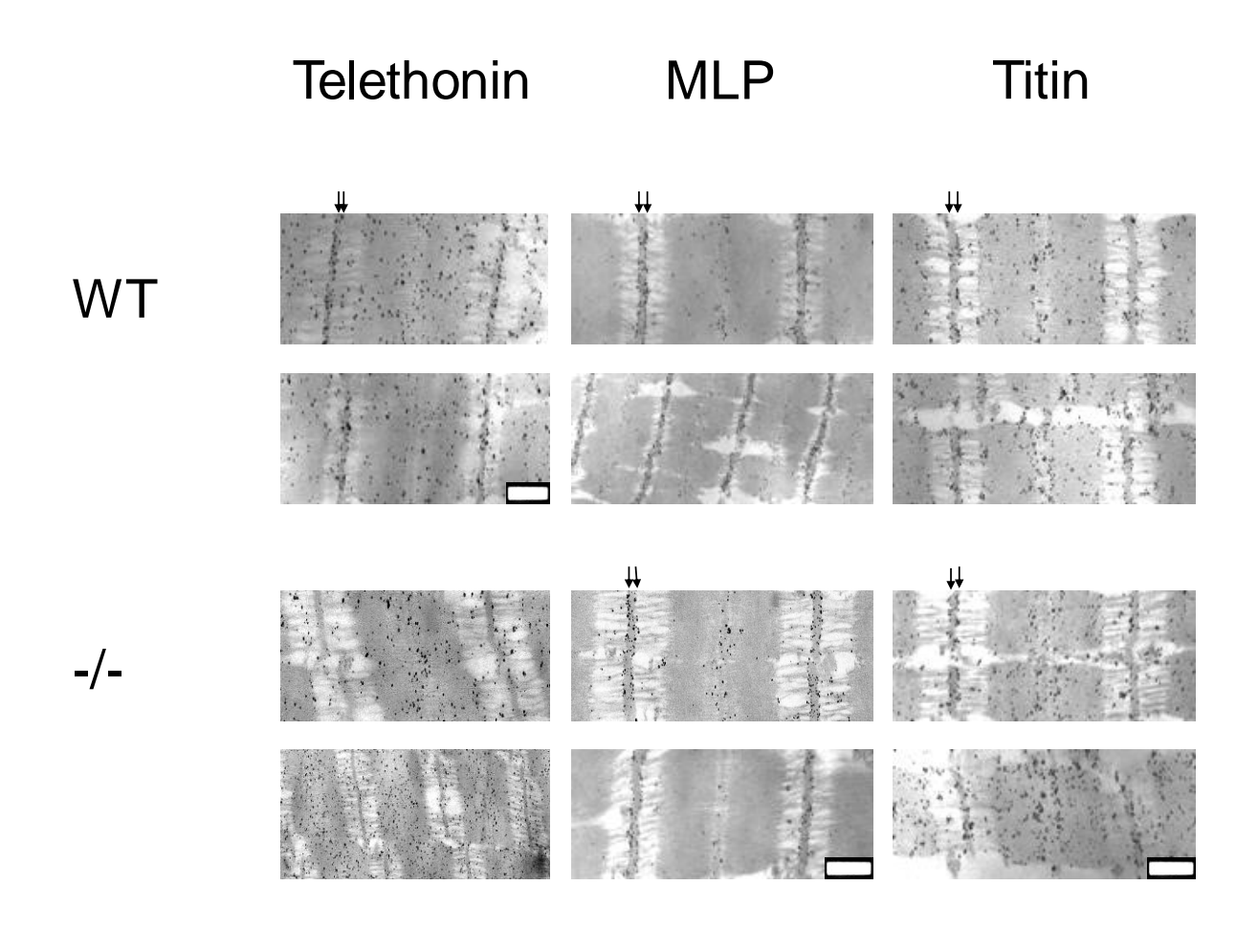


Online Figure II: Epifluorescence measurements of intracellular Ca2+ handling

Original Ca2+ transients (a) and summary data (b) of wildtype (WT, n=14 cells from 7 mice) or homozygous telethonin-deficient (KO, n=12 from 8) mice showing Ca2+ transients and Ca2+ decay (c). SR Ca load assessed by post-rest-potentiation (d) and caffeine-induced Ca2+ transients (e) as well as Na+/Ca2+ exchange function (NCX, f) show unaltered Ca2+metabolism in the KO

2

1



4

5

- 6 Online Figure III: Immunogold electron microscopy
- 7 Remarkably normal Z-disks were observed, even if telethonin is missing (upper 2 rows:
- 8 wildtype, lower 2 rows telethonin knock out tissue). The white part of the scale bar represents
- 9 500 nm.

1 Online Figure IV

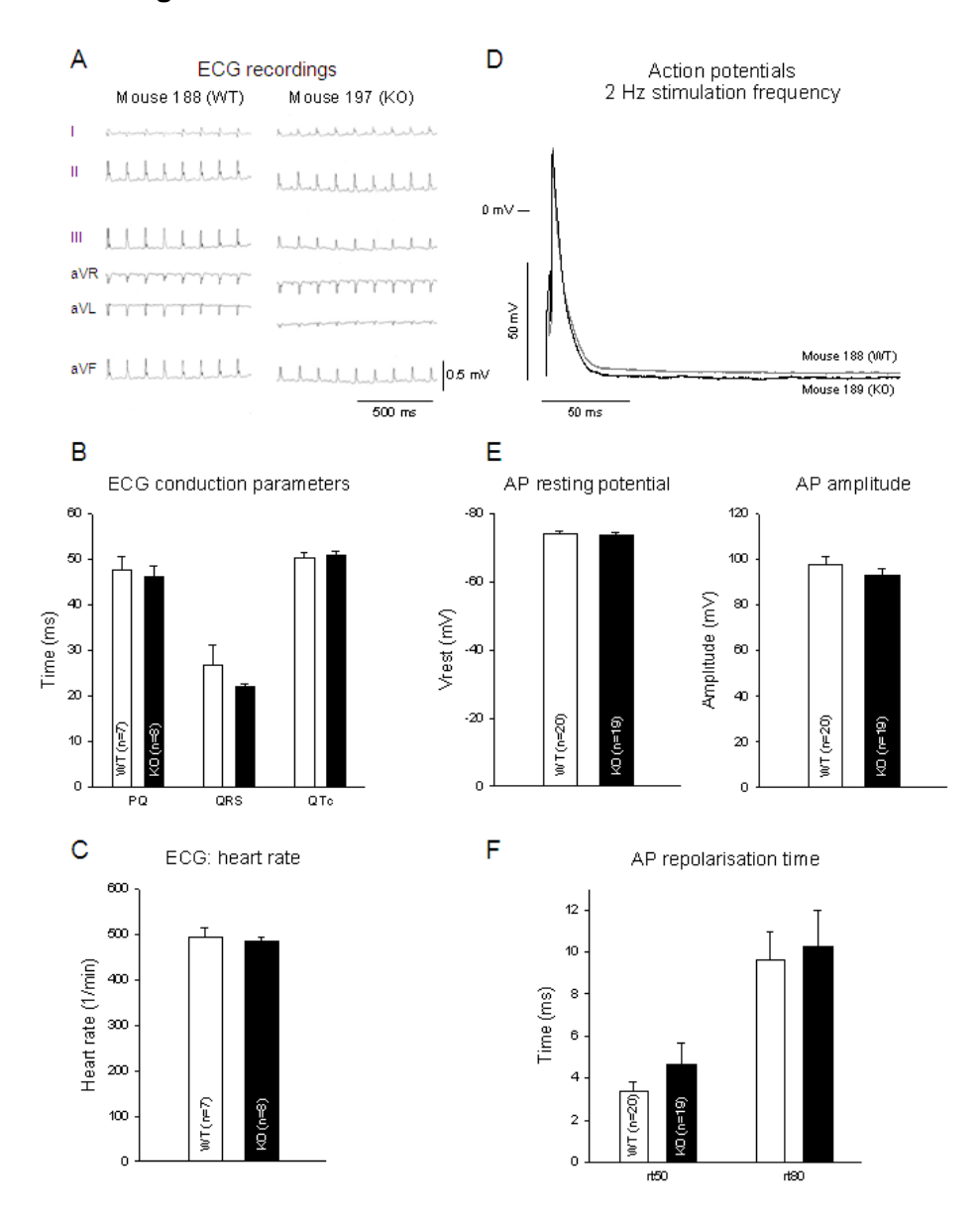
2

3

4

5

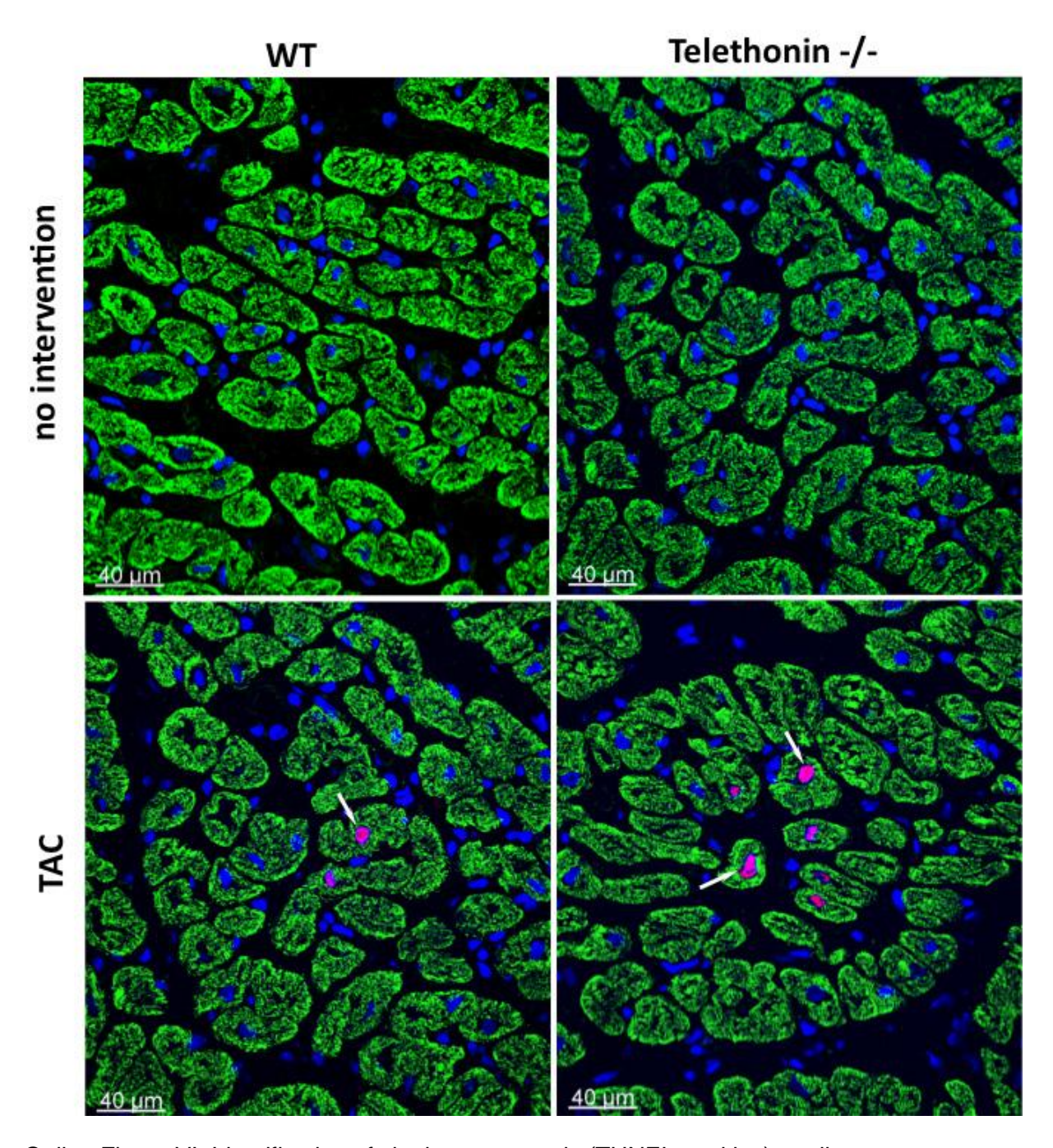
6 7



Online Figure IV: Electrocardiograms (ECG) and action potential measurements

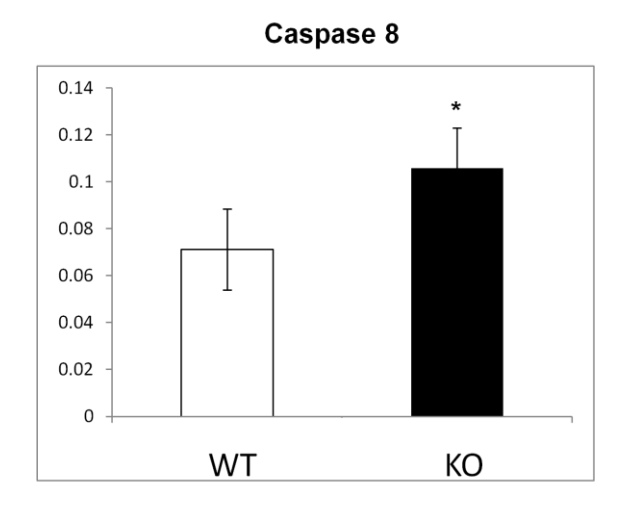
Original ECG recordings (A) and summary of conduction parameters (B) and heart rate (C) in wildtype (WT, n=7) or homozygous telethonin-deficient (KO, n=8) mice. Original action potential recordings (D) and summary of action potential parameters (E & F).

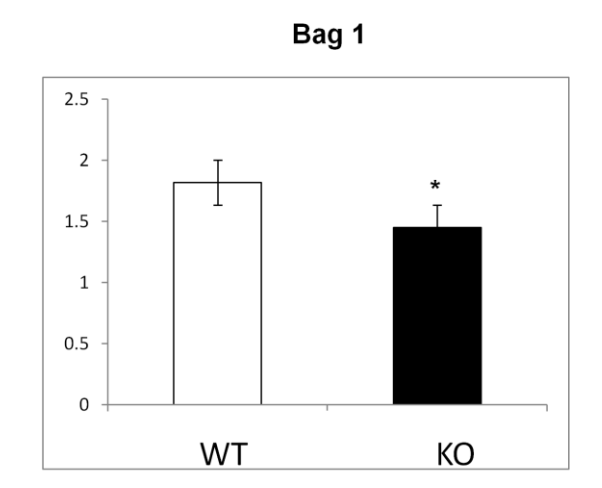
1 Online Figure V



- 3 Online Figure VI: Identification of single apoptoptotic (TUNEL positive) cardiac myocytes.
- 4 The arrows identify single TUNEL positive cardiac myocytes (blue: DAPI, green: F-actin,
- 5 pink: TUNEL positive nuclei).

1 Online Figure VI



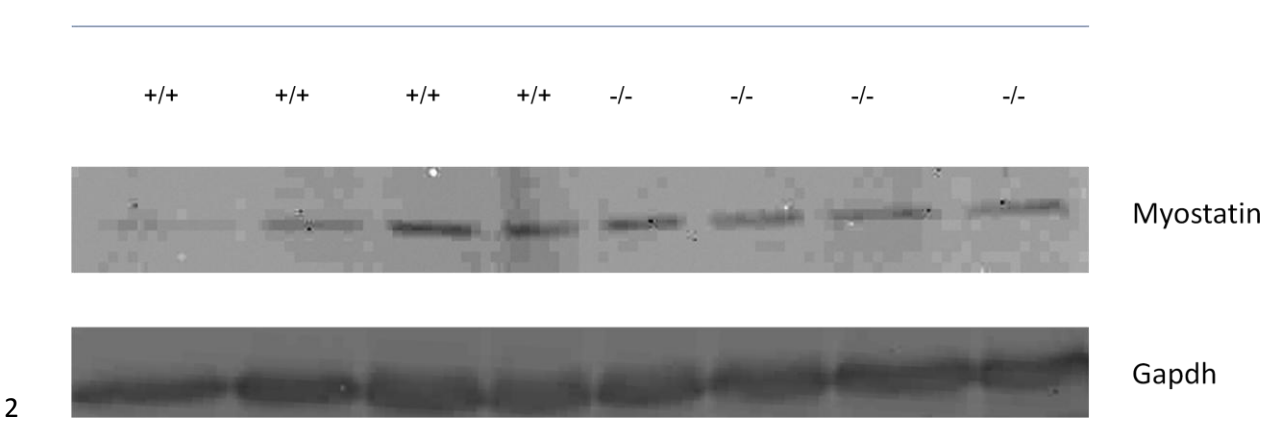




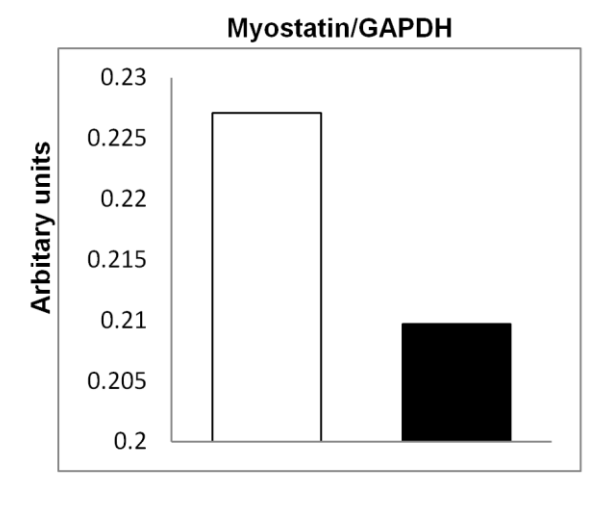
Online Figure VI: Analysis of apoptotic gene expression in telethonin deficient animals following TAC. Caspase 8 is a target gene of $p53^{11}$ and important in the execution of the apoptosis pathway. Bcl2-associated athanogene 1 (Bag1) has anti-apoptotic effects and is downregulated in telethonin knockout animals after TAC. (Data are obtained from the SA Biosciences apoptosis gene expression array and are normalized to glucoronidase beta (Caspase 8) or to hypoxanthine guanine phosphoribosyl transferase 1 (Bag1)); * = p<0.05).

1 Online figure VII

Transverse aortic constriction (TAC)



3



WT n = 4

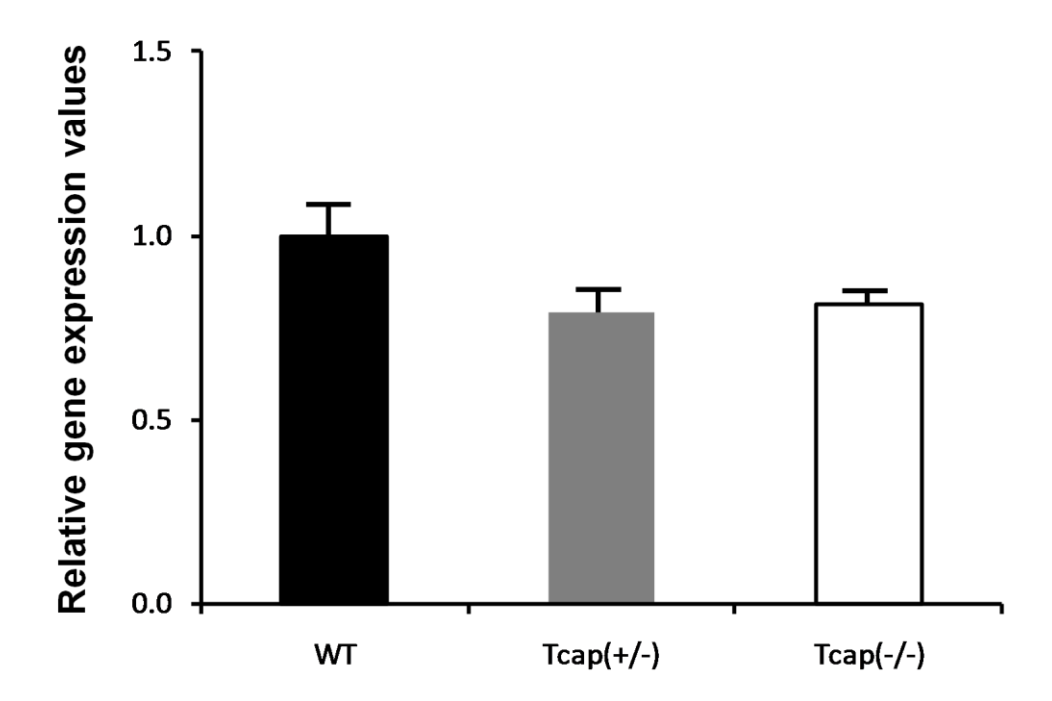
4 5

6

7

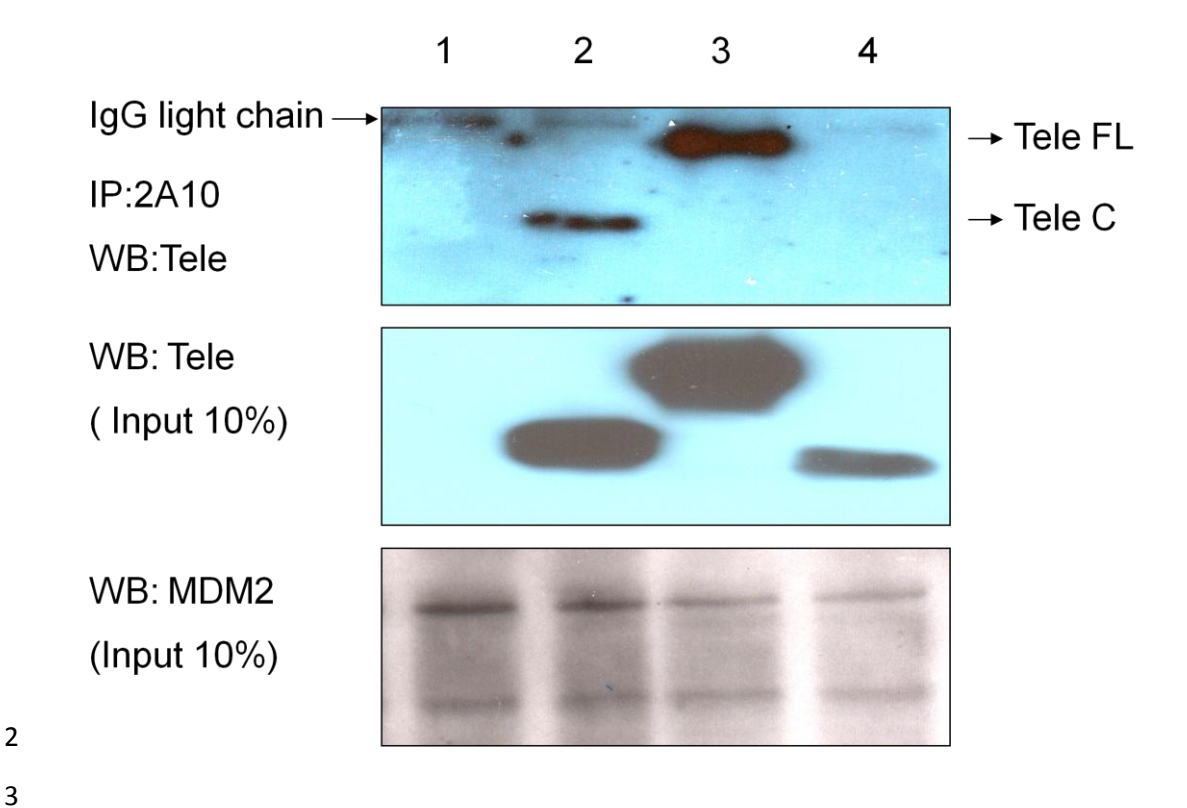
8 9 Online figure VII: Analysis of myostatin protein expression in telethonin knockout animals after TAC. We did not detect any significant change in myostatin protein expression following biomechanical stress in form of transverse aortic constriction in the telethonin knockout animals (Graph).

1 Online figure VIII



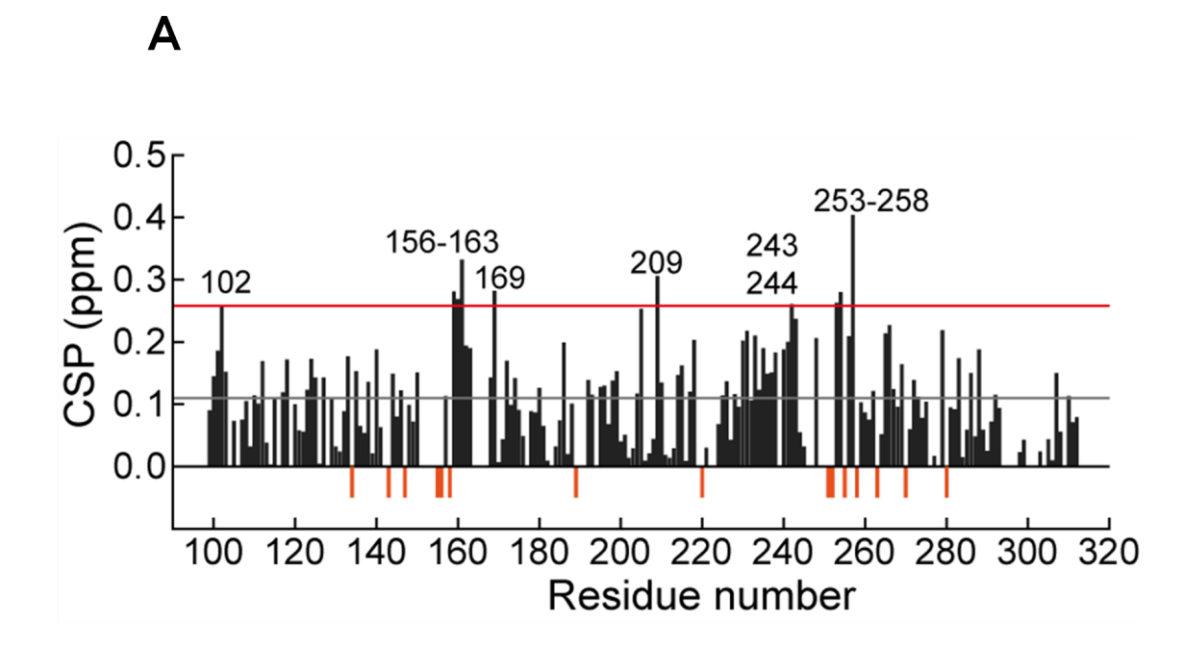
Online figure VIII: Analysis of myostatin mRNA expression in telethonin knockout animals after TAC. We did not detect any change in myostatin mRNA expression following biomechanical stress in form of transverse aortic constriction in telethonin heterozygous or homozygous knockout animals (between 5 and 10 animals per group).

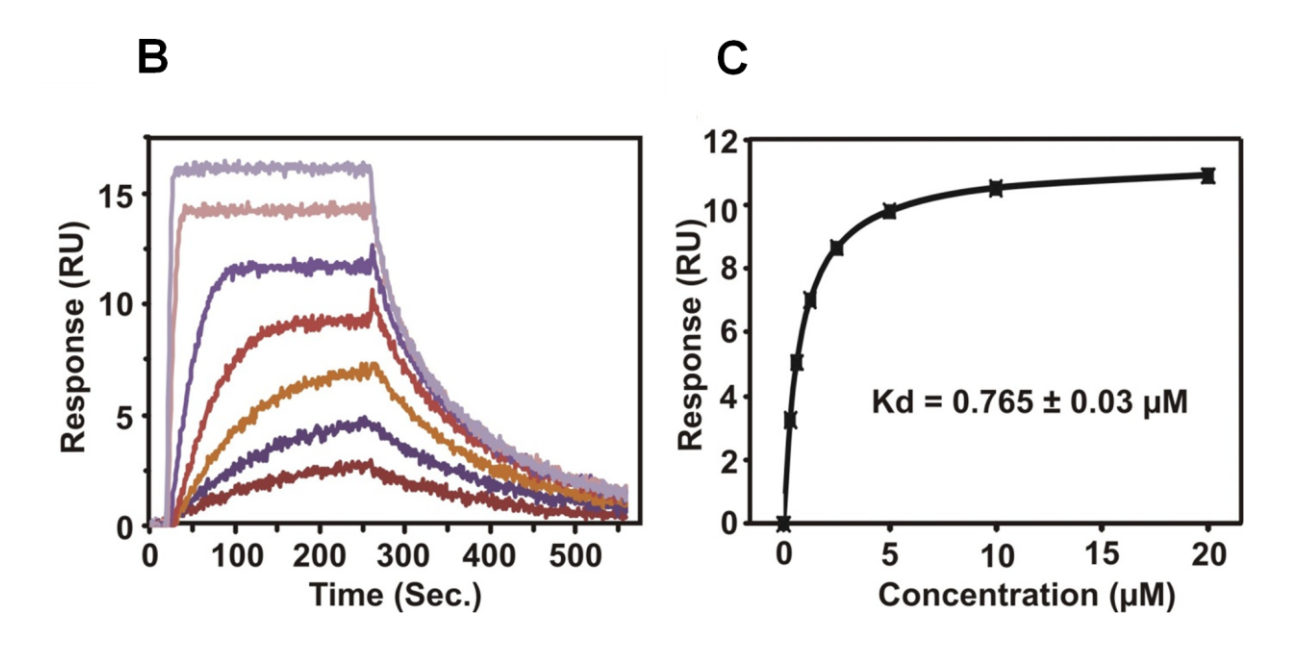
1 Online Figure IX



Online Figure IX: Telethonin (Tele) interacts with MDM2. Lane1: non transfected, lane 2: HA-telethonin carboxyterminus (C), lane 3 HA-telethonin full length (FL), lane 4 HA-telethonin aminoterminus (N), 2A10 is an anti-MDM2 antibody

1 Online Figure X



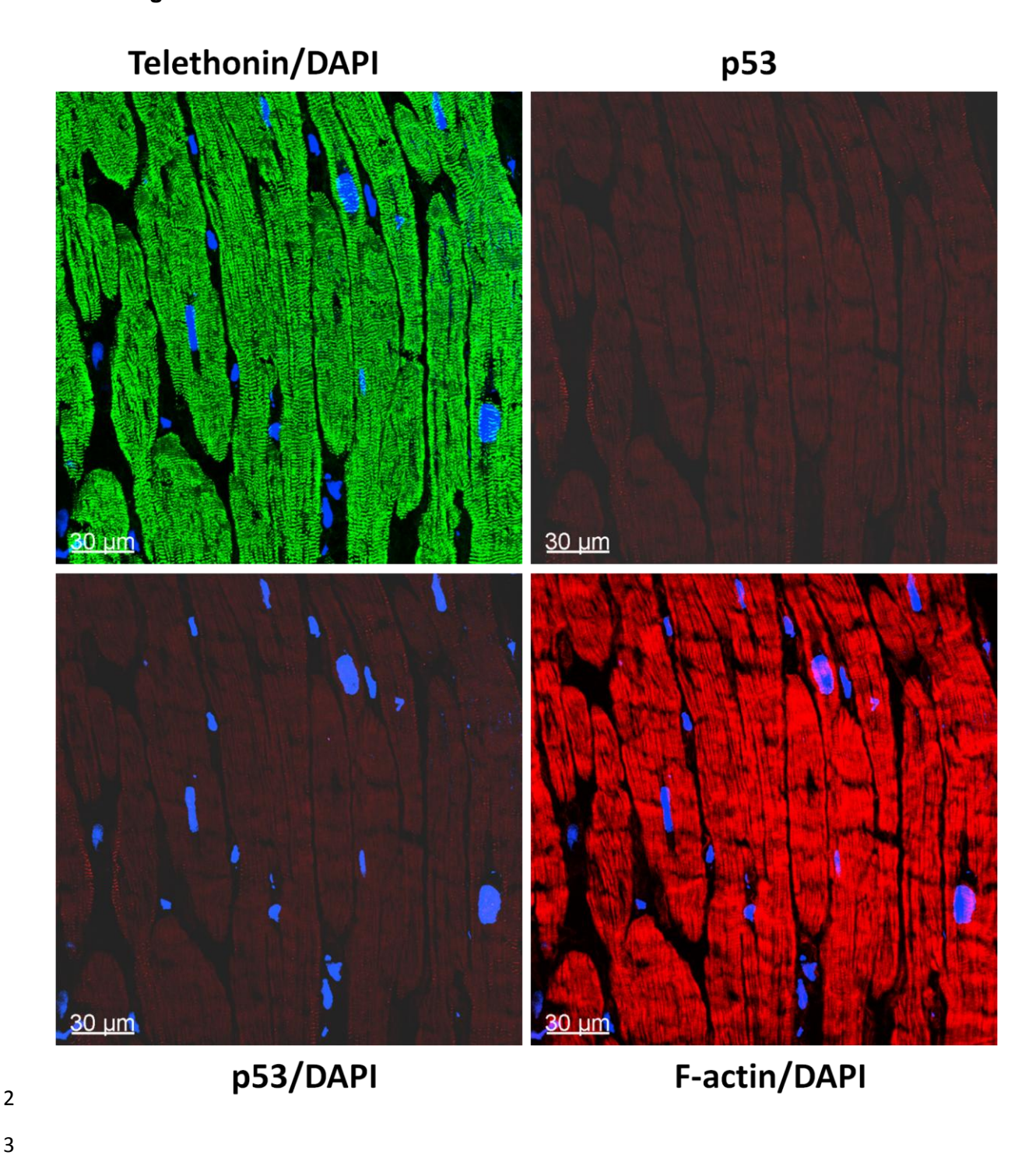


Online Figure X: NMR spectroscopy and Biacore assay monitoring p53-DBD binding to telethonin. (A) NMR chemical shift perturbation (CSP) of the 1H , ^{15}N NMR signals comparing 50 μ M p53DBD free and in the presence of telethonin. Gray and red lines indicate the mean value and the mean plus two times the standard deviation, respectively. Red negative bars represent residues whose corresponding signals disappeared upon complex formation. (B) Biosensograms of different concentrations (from bottom to top: 0.31, 062, 1.25, 2.5, 5, 10, 20 μ M) of p53 binding to full-length telethonin (1-167); (C) The binding affinity (fitted to an apparent 1:1 stoichiometry) was calculated from plotting the equilibrium binding response versus different concentrations of p53DBD.

1 Online Figure XI

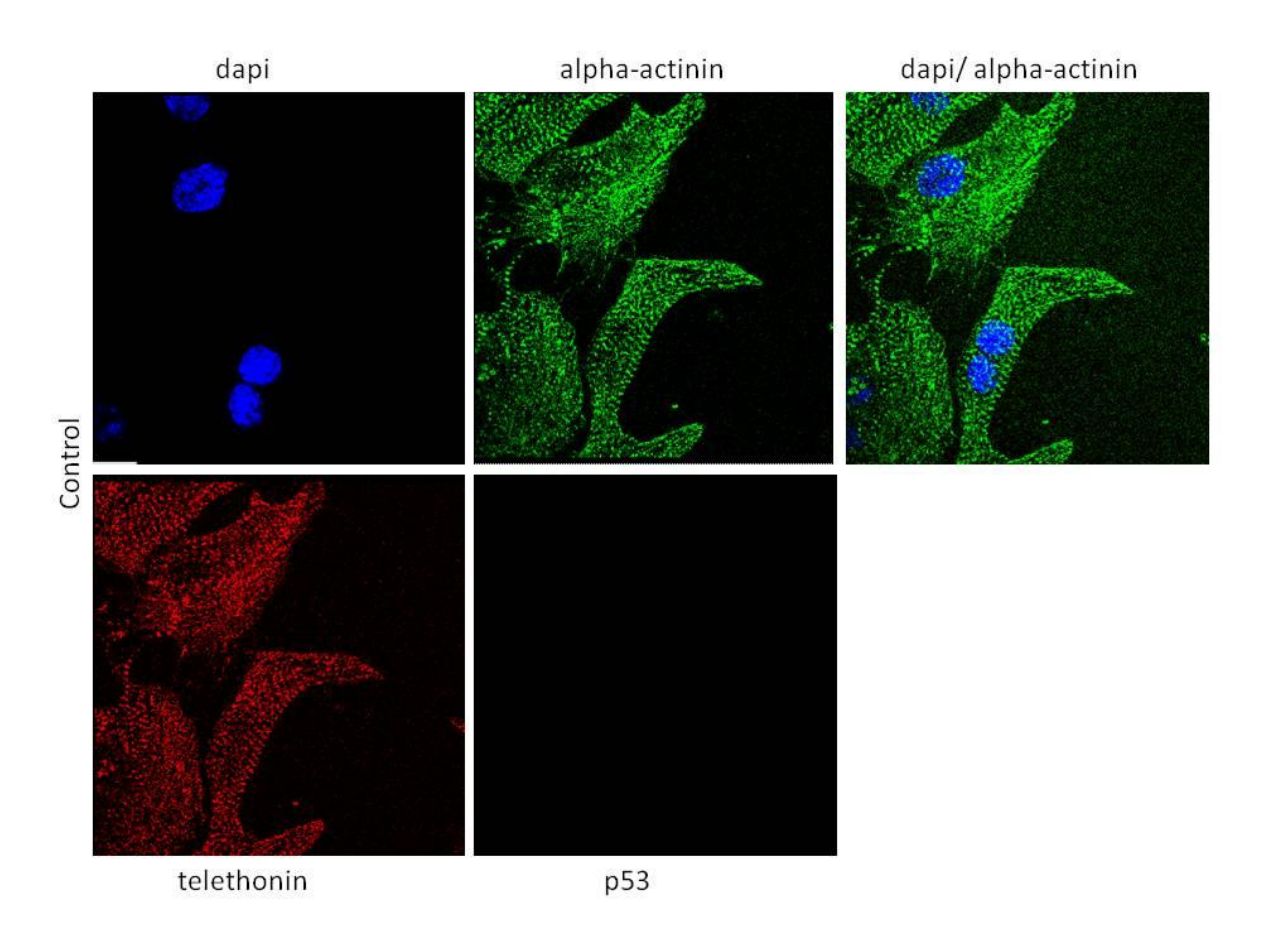
4 5

6



Online Figure XI: Localization of telethonin and p53 in wildtype animals under spontaneous conditions. Whereas telethonin is localized at the sarcomeric Z-disk, p53 can't be detected at all. Cardiomyocytes are identified by their typical cross striated pattern (Z-disks) as indicated by telethonin staining and f-actin labeling.

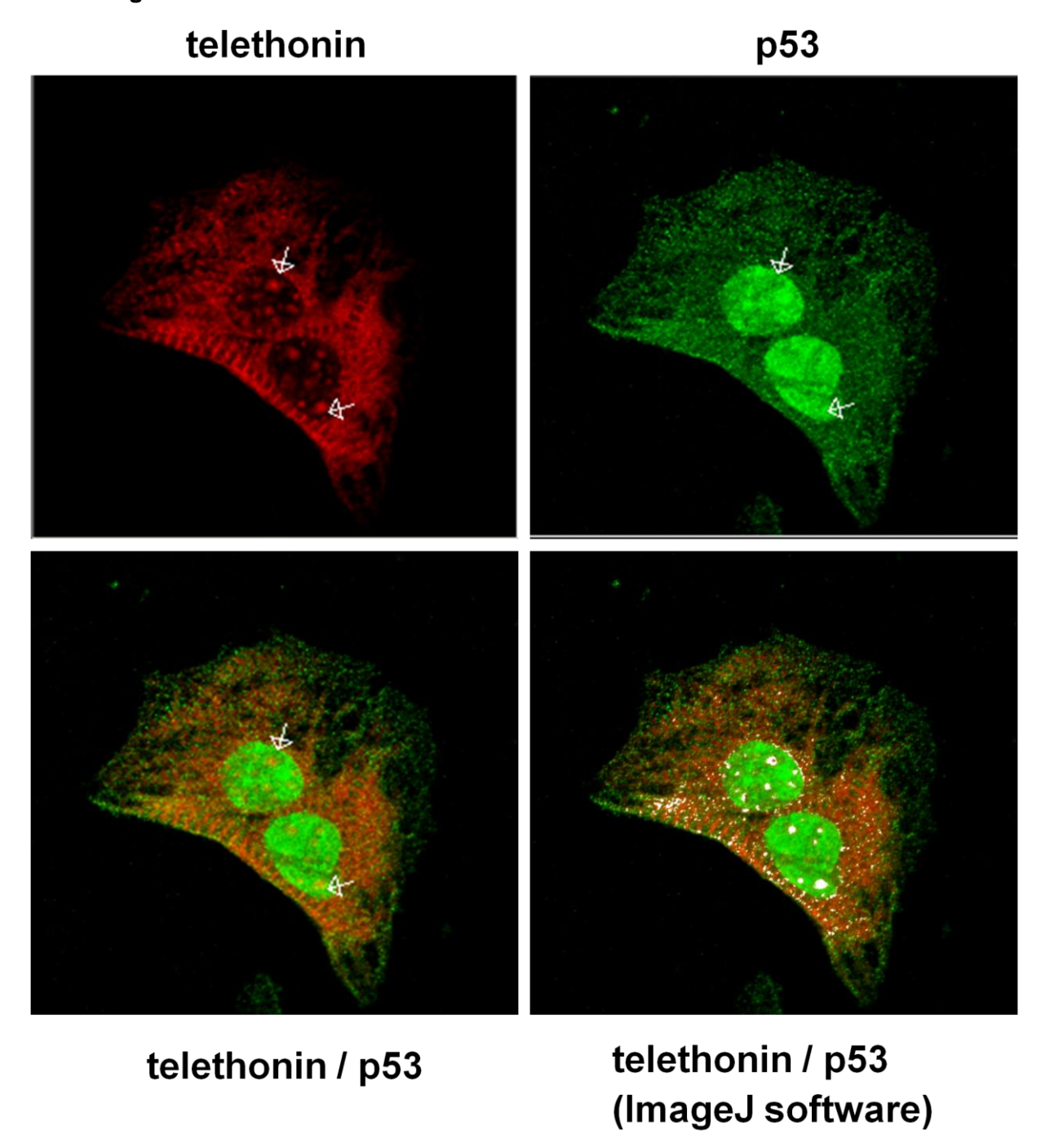
1 Online Figure XII



Online Figure XII: Localization of telethonin and p53 in neonatal rat cardiomyocytes. For these studies, cells were fixed and incubated with rat polyclonal anti-telethonin antibody, rabbit polyclonal anti-p53 (FL393,SantaCruz), and mouse monoclonal anti-alpha actinin(Sigma). The secondary antibodies used were anti-rat Alexa-labeled 633, anti-mouse Alexa-labeled 488 and anti-rabbit Alexa-labeled 555 (Invitrogen).

Cardiomyocytes are identified by their typical cross striated pattern (Z-disks) as indicated by alpha-actinin and telethonin staining. Telethonin is localized at the Z-disks, but p53 is undetectable in untreated neonatal rat cardiomyocytes.

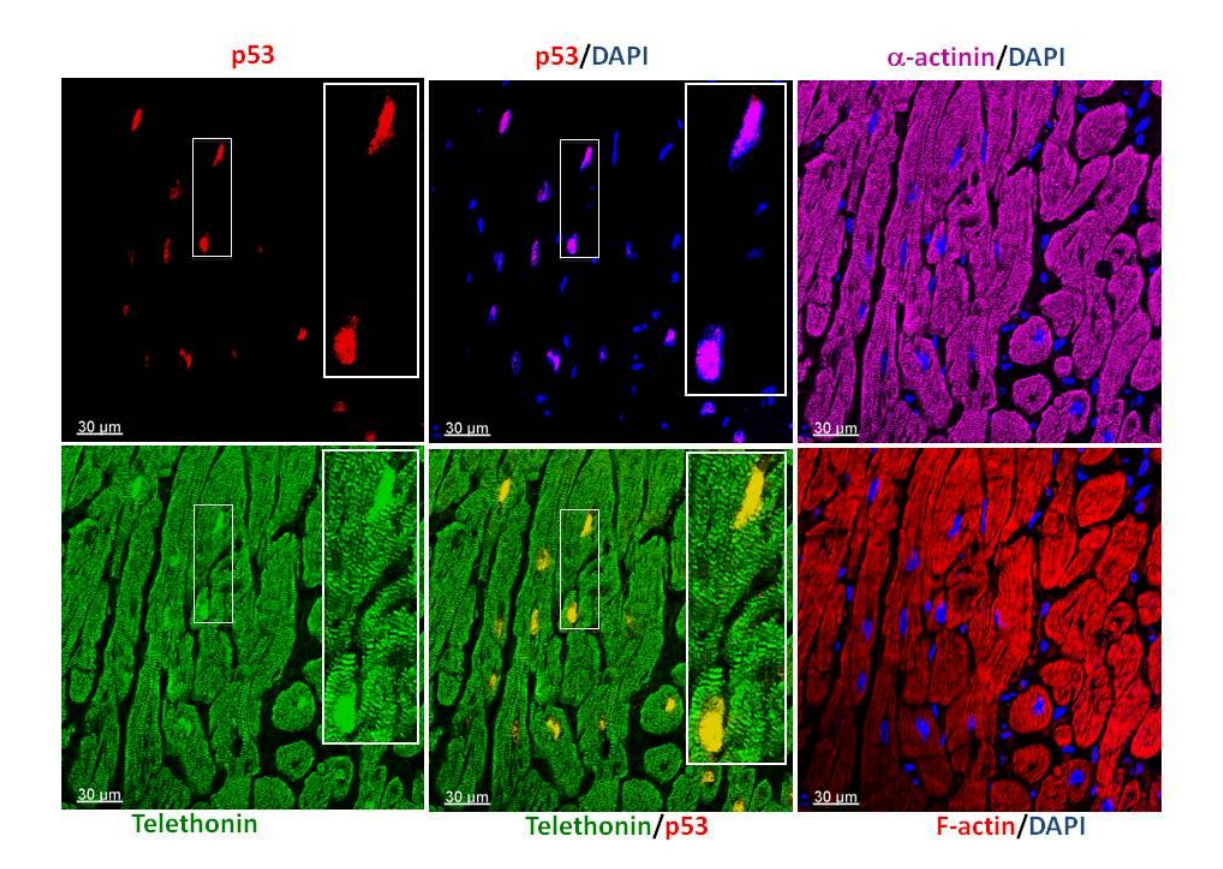
1 Online Figure XIII



Online Figure XIII: Colocalization of telethonin and p53 after doxorubicin treatment of cells. For the colocalization studies, neonatal rat cardiomyocytes were treated with doxorubicin (1µM,Sigma) for 24 hours, fixed and incubated with rat polyclonal anti-telethonin antibody, rabbit polyclonal anti-p53 (FL393,SantaCruz)and/or mouse monoclonal p53 (1C12,Cell signaling). The secondary antibodies used were anti-rat Alexa-labeled 633, anti-rabbit Alexa-labeled 488 and / or anti mouse Alexa labeled 488.

Arrows indicate nuclear localization of telethonin (upper left and right panels), or telethonin/p53 colocalization(confocal microscopy, lower left panel). ImageJ software (http://rsbweb.nih.gov/ij/) was used to identify colocalization as well. Cardiomyocytes are identified by their typical cross striated pattern (Z-disks) as indicated by telethonin staining.

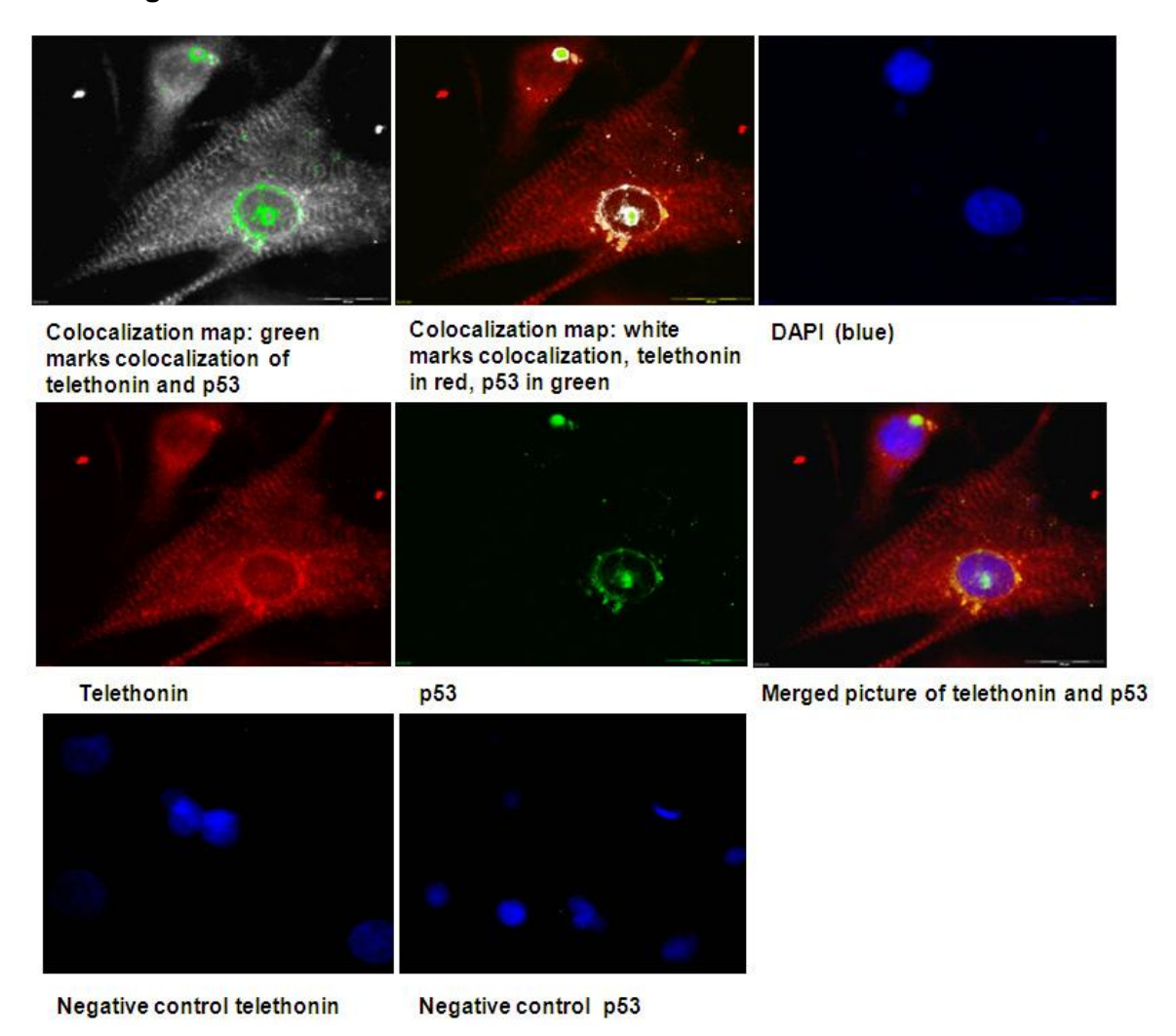
1 Online Figure XIV



Online Figure XIV: Colocalization of telethonin and p53 after doxorubicin treatment of animals. To induce heart failure, doxorubicin was administered by surgical implantation of a mini-osmotic pump (Alzet). Using this model, doxorubicin was administered at 0.5 microliter per hour for 21 days resulting in a cumulative dose of 126 microgram.

Representative confocal micrographs showing nuclear localization of p53 in doxorubicin treated animals. Note that in these mice, telethonin is present in the nuclei where it colocalizes with p53. Inserts are higher magnifications of the boxed regions.

1 Online Figure XV



Online Figure XV: Colocalization of GFP-telethonin with p53 in neonatal rat cardiomyocytes. Neonatal rat cardiac myocytes were transfected with a GFP-telethonin construct and colocalization was monitored using an Olympus FluoView 1000 Confocal microscope; 488nm, 544nm (multiline) and 633nm laser-lines. Colocalization was analyzed via ImageJ Software (Wayne Rasband, Version 1.410; Modul "Colocalization Finder" by Christophe Laummonerie, Jerome Mutterer, Institut de Biologie Moleculaire des Plantes, Strasbourg, France).

1 Online Tables:

	Spontaneous phenotype		
	WT (n=15)	het (n=10)	-/- (n=14)
Septum Width	1.06 +/- 0.12	1.02 +/- 0.12	1.00 +/- 0.10
Enddiastol. Diameter (mm)	3.8 +/- 0.3	3.9 +/- 0.4	3.8 +/- 0.5
Posterior Wall (mm)	1.06 +/- 0.16	1.03 +/- 0.12	1.0 +/- 0.1
Endsystol. Diameter (mm)	2.4+/- 0.4	2.5+/- 0.5	2.6+/- 0.4
Fractional-Shortening (%)	36.2 +/- 6.8	35.5 +/- 7.3	31.5 +/- 5.3
HR	441.1 +/-53.9	450.1 +/-59.1	386.5 +/-54.2

- 2
- 3 Online Table I: Echocardiography of the spontaneous phenotype of telethonin knockout, telethonin
- 4 heterozygous, and wildtype littermates. Please note: no significant differences were observed
- 5 between telethonin knock out and wildtype animals under basal conditions.
- 6 (HR = heart rate; WT = wildtype, het = heterozygous, -/- = homozygous knock out)

	NTG (n=32)	TG (n=26)
Septum Width	0,80±0,08	0,78±0,09
Enddiastol. Diameter (mm)	4,07±0,29	4,01±0,39
Posterior Wall (mm)	0,78±0,08	0,78±0,09
Endsystol. Diameter (mm)	2,91±0,32	2,84±0,45
Fractional-Shortening (%)	28,65±5,93	29,48±6,64
HR	517,72±36,32	505,77±45,54

- 7
- 8 Online Table II: Echocardiography of the spontaneous phenotype of telethonin transgenic (i. e.
- 9 telethonin overexpressing animals). Please note: no significant differences were observed between
- 10 transgenic and wildtype litter mate control animals under basal conditions. (HR = heart rate, NTG =
- non transgenic wildtype control animals, TG = transgenic animals)

References

2

1

- 1. Hu P, Zhang D, Swenson L, Chakrabarti G, Abel ED, Litwin SE. Minimally invasive aortic banding in mice: effects of altered cardiomyocyte insulin signaling during pressure overload. *Am J Physiol Heart Circ Physiol*. 2003;285:H1261-1269.
- Knöll R, Hoshijima M, Hoffman HM, Person V, Lorenzen-Schmidt I, Bang ML, Hayashi T, Shiga N, Yasukawa H, Schaper W, McKenna W, Yokoyama M, Schork NJ, Omens JH, McCulloch AD, Kimura A, Gregorio CC, Poller W, Schaper J, Schultheiss HP, Chien KR. The cardiac mechanical stretch sensor machinery involves a Z disc complex that is defective in a subset of human dilated cardiomyopathy. *Cell.* 2002;111:943-955.
- 11 3. Carrier L, Knoll R, Vignier N, Keller DI, Bausero P, Prudhon B, Isnard R, Ambroisine ML, 12 Fiszman M, Ross J, Jr., Schwartz K, Chien KR. Asymmetric septal hypertrophy in 13 heterozygous cMyBP-C null mice. *Cardiovascular research*. 2004;63:293-304.
- 4. Maier LS, Zhang T, Chen L, DeSantiago J, Brown JH, Bers DM. Transgenic CaMKIIdeltaC overexpression uniquely alters cardiac myocyte Ca2+ handling: reduced SR Ca2+ load and activated SR Ca2+ release. *Circ Res.* 2003;92:904-911.
- Wagner S, Dybkova N, Rasenack EC, Jacobshagen C, Fabritz L, Kirchhof P, Maier SK, Zhang T,
 Hasenfuss G, Brown JH, Bers DM, Maier LS. Ca2+/calmodulin-dependent protein kinase II
 regulates cardiac Na+ channels. J Clin Invest. 2006;116:3127-3138.
- 20 6. Opitz CA, Kulke M, Leake MC, Neagoe C, Hinssen H, Hajjar RJ, Linke WA. Damped elastic recoil of the titin spring in myofibrils of human myocardium. *Proc Natl Acad Sci U S A.* 2003;100:12688-12693.
- Linke WA, Rudy DE, Centner T, Gautel M, Witt C, Labeit S, Gregorio CC. I-band titin in cardiac muscle is a three-element molecular spring and is critical for maintaining thin filament structure. *J Cell Biol.* 1999;146:631-644.
- 26 8. Zou P, Gautel M, Geerlof A, Wilmanns M, Koch MH, Svergun DI. Solution scattering suggests cross-linking function of telethonin in the complex with titin. *J Biol Chem.* 2003;278:2636-2644.
- Zou P, Pinotsis N, Lange S, Song YH, Popov A, Mavridis I, Mayans OM, Gautel M, Wilmanns
 M. Palindromic assembly of the giant muscle protein titin in the sarcomeric Z-disk. *Nature*.
 2006;439:229-233.
- 32 10. Hagn F, Klein C, Demmer O, Marchenko N, Vaseva A, Moll UM, Kessler H. BclxL changes 33 conformation upon binding to wild-type but not mutant p53 DNA binding domain. *J Biol Chem.* 2010;285:3439-3450.
- Ehrhardt H, Hacker S, Wittmann S, Maurer M, Borkhardt A, Toloczko A, Debatin KM, Fulda
 S, Jeremias I. Cytotoxic drug-induced, p53-mediated upregulation of caspase-8 in tumor
 cells. Oncogene. 2008;27:783-793.